

2014

Characterization and Development of an Extended Cavity Tunable Laser Diode

Fnu Traptilisa
San Jose State University

Follow this and additional works at: http://scholarworks.sjsu.edu/etd_theses

Recommended Citation

Traptilisa, Fnu, "Characterization and Development of an Extended Cavity Tunable Laser Diode" (2014). *Master's Theses*. Paper 4441.

This Thesis is brought to you for free and open access by the Master's Theses and Graduate Research at SJSU ScholarWorks. It has been accepted for inclusion in Master's Theses by an authorized administrator of SJSU ScholarWorks. For more information, please contact scholarworks@sjsu.edu.

CHARACTERIZATION AND DEVELOPMENT OF AN EXTENDED CAVITY
TUNABLE LASER DIODE

A Thesis

Presented to

The Faculty of the Department of Physics and Astronomy
San José State University

In Partial Fulfillment

of the Requirements for the Degree

Master of Science

by

Fnu Traptilisa

May 2014

© 2014

Fnu Traptilisa

ALL RIGHTS RESERVED

The Designated Thesis Committee Approves the Thesis Titled

CHARACTERIZATION AND DEVELOPMENT OF AN EXTENDED CAVITY
TUNABLE LASER DIODE

by

Fnu Traptilisa

APPROVED FOR THE DEPARTMENT OF PHYSICS AND ASTRONOMY

SAN JOSÉ STATE UNIVERSITY

May 2014

Dr. Peter Beyersdorf	Department of Physics and Astronomy
Dr. Ramendra Bahuguna	Department of Physics and Astronomy
Dr. Kenneth Wharton	Department of Physics and Astronomy

ABSTRACT

CHARACTERIZATION AND DEVELOPMENT OF AN EXTENDED CAVITY TUNABLE LASER DIODE

by Fnu Traptilisa

A laser diode emits a narrow range of frequencies. However, drifts in frequency occur over time due to many factors like changes in laser temperature, current, mechanical vibrations in the apparatus, etc. These frequency drifts make the laser unsuitable for experiments that require high frequency stability. We have used an atomic transition in rubidium as a frequency reference and used Doppler free saturated spectroscopy to observe the reference peak. We have designed an electronic locking circuit that operates the diode laser at a specific frequency. It keeps the laser at that frequency for a long period of time with very few or no drifts.

We have constructed and characterized an extended cavity diode laser that costs significantly less than a commercial unit. It is much more compact with performance comparable to that of a commercial unit. It can be used in undergraduate and graduate optics laboratories where commercial units are cost prohibitive. The various components of the set-up are discussed, and the basic principles behind the function and operation of this versatile device are explained. We designed a servo loop filter circuit, which is used to stabilize the frequency of the laser to an atomic reference frequency. We also generated an error signal using a technique similar to the Pound Hall Drever technique and then feedback the error signal in the loop filter circuit.

DEDICATION

To my Family and Friends

ACKNOWLEDGEMENTS

The success of this project depends largely on the encouragement and guidelines of many people. I take this opportunity to express my gratitude to the people who have been instrumental in the successful completion of this project.

I would like to express my very great appreciation to the committee members and professors in the department of Physics and Astronomy at San Jose State University for their patient guidance, enthusiastic encouragement and useful critiques of this research work.

Special thanks should be given to Dr. Peter Beyersdorf, my research project supervisor, for his professional guidance and valuable support. His willingness to motivate me contributed tremendously to my project. His constructive recommendations on this project have helped me in acquiring useful laboratory skills. I consider this project a great opportunity for me to work with and learn from a mentor like him.

I would also like to thank all of my family and friends who supported me in writing, and motivated me to strive towards my goal. Finally, I wish to thank my husband Anshul Kumar for his support and encouragement throughout my study.

TABLE OF CONTENTS

CHAPTER

1	SEMICONDUCTOR LASER DIODE	1
1.1	Introduction	1
1.2	Fundamentals of Laser Operation	1
1.2.1	Absorption, Spontaneous and Stimulated Emission	1
1.2.2	Population Inversion and Pumping	3
1.2.3	Optical Resonators	3
1.3	Semiconductor Laser Diode	4
1.4	Basic Characteristics of a Semiconductor Laser Diode	6
1.4.1	Threshold current and threshold current density	6
1.4.2	Output Power	8
1.4.3	Beam Divergence and Astigmatism	9
1.4.4	Optical Spectrum	10
1.4.5	Center Wavelength Change with Temperature	12
1.4.6	Mode Hopping	12
1.5	Types of Semiconductor Diode Laser	13
1.5.1	Double Heterostructure Diode Laser	13
1.5.2	Quantum Well Diode Laser	14
1.5.3	Quantum Cascade Diode Laser	14
1.5.4	Separate Confinement Heterostructure Diode Laser	14
1.5.5	Other Types of Diode Lasers	15

2	EXTENDED CAVITY DIODE LASER	16
2.1	Introduction	16
2.2	Design of an Extended Cavity Diode Laser	17
2.2.1	Littrow Cavity Configuration	18
2.3	Components and Parts of an ECDL	20
2.4	Operating Principle of an ECDL	23
2.5	Alignment of an ECDL	24
2.6	Calibration of an ECDL: Mode-Hop Suppression	26
3	FREQUENCY TUNING PARAMETERS OF THE ECDL	30
3.1	Introduction	30
3.2	First Tuning Parameter- Temperature	30
3.3	Second Tuning Parameter- Injection Current	31
3.4	Third Tuning Parameter- Grating Optical Feedback	32
3.5	Data Collection and Analysis	33
3.5.1	Mach Zehnder Interferometer	33
4	ATOMIC SPECTROSCOPY- RUBIDIUM CELL	39
4.1	Introduction	39
4.2	Basic Concept of Frequency Stabilization	39
4.3	Monitoring the Laser Frequency	40
4.4	Rubidium Vapor Cell	41
4.4.1	Fine Structure Levels	42
4.4.2	Hyperfine Levels	44
4.4.3	Transitions	45
4.5	Doppler Broadened Absorption Spectra	45
4.6	Saturated Absorption Spectroscopy	47

5	ELECTRONIC LOCKING CIRCUIT	50
5.1	Introduction	50
5.2	Generating an Error Signal	51
5.2.1	Frequency Modulation	51
5.2.2	Demodulation	54
5.3	Design of the Electronic Feedback Circuit	54
5.3.1	Feedback Loop Filter	55
5.3.2	Loop Filter Electronics	58
5.4	Locking the Laser and Loop Optimization	61
5.5	Printed Circuit Board (PCB)	63
6	RESULTS AND CONCLUDING REMARKS	66
6.1	Results	66
6.2	Concluding Remarks and Future Work	68
	BIBLIOGRAPHY	70
	APPENDIX	
A	PRINTED CIRCUIT BOARD	72

LIST OF FIGURES

Figure

1.1	Three types of transitions (a) Resonant absorption, (b) Spontaneous emission, (c) Stimulated emission.	2
1.2	Energy level diagram for an atom and a crystal.	5
1.3	Energy bands in semiconductors.	6
1.4	Output light versus injection current in a semiconductor diode laser(reprinted with permission from Newport tutorial).	8
1.5	Structure and lasing mode in a semiconductor laser.	9
1.6	Multimode versus single mode spectra (reprinted with permission from Newport tutorial).	10
1.7	Geometry of a linear laser cavity.	11
1.8	Mode hopping observed while temperature tuning a laser diode (reprinted with permission from Newport tutorial).	12
2.1	Tunable external cavity diode laser with (a) Littrow and (b) Littman configuration.	18
2.2	Littrow configuration set up.	19
2.3	Blazed grating.	20
2.4	Extended Cavity Diode Laser (ECDL) set up.	21
2.5	Pin hole alignment technique, G: grating, P: piece of paper with a pin hole, M2: mirror attached inside the mount parallel to the grating, M1: external mirror, LD: laser diode.	25

2.6	L-I curve.	26
2.7	Different ways to move the grating and the corresponding change in wavelength.	27
2.8	Schematic diagram of laser configuration showing optimum rotation point R, LD: laser diode, G: grating.	29
3.1	Tuning the wavelength with the grating.	33
3.2	Mach Zehnder interferometer set up, LD-laser diode, BS-beam splitter, L-Lens, M-mirror, PD-photodiode, OSC-oscilloscope, CCD-Camera. .	34
3.3	Mach Zehnder interference pattern showing frequency change with PZT voltage, the top blue signal shows interference fringes and the bottom one is PZT voltage.	36
3.4	Mach Zehnder interference pattern seen through a CCD camera. . . .	37
4.1	Rubidium vapor cell.	41
4.2	Energy manifold of rubidium D2 transition.	44
4.3	Experimental set up of rubidium spectroscopy.	46
4.4	Doppler broadened rubidium absorption spectrum.	46
4.5	Optical set up for rubidium saturated spectroscopy: LD-laser diode, LDC-laser diode controller, PZT- piezoelectric transducer, CH- chopper, M-mirror, BS-beam splitter, PD-photodiode, OSC- oscilloscope, OSA-optical spectrum analyser, Rb cell-rubidium cell, lock-in-Amp- Lock in Amplifier.	49
4.6	Doppler free rubidium absorption spectrum, the top yellow trace shows a dip in the absorption spectral line and the bottom blue trace is the amplified signal from the lock-in amplifier.	49

5.1	RF signal injection to the laser diode current controller.	52
5.2	Error signal using frequency modulation, (a) power versus frequency plot showing an absorption line, (b) shape of an error signal.	53
5.3	Set up for generating an error signal, LD: laser diode, PD: photodiode, Rb cell: rubidium cell, RF: radio-frequency, LPF: Low pass filter. . .	53
5.4	Loop filter circuit - The switches SW3 and SW5 are used for increasing the DC gain, and the switches SW2 and SW6 are used to rapidly turn the servo on and off. The offset on the second stage amplifier is used to bias the output such that the unlocked laser is not perturbed by the circuit.	56
5.5	Bode plot for the feedback loop filter circuit.	57
5.6	Printed circuit board for the feedback loop filter circuit.	64
5.7	Bode gain plot for opamp U1 with SW3 closed.	65
5.8	Bode gain plot for opamp U3 with SW5 closed.	65
6.1	The yellow signal (top) is an error signal, the blue signal (bottom) is the resonance of an Rb cell.	66
6.2	Laser frequency locking: transmitted light intensity versus time, rep- resenting a lock duration of 9 seconds.	67
6.3	New ECDL mount that reduces mode-hop.	69
A.1	PCB Board (a) front panel and (b) back panel.	72
A.2	Board layout with traces.	73

CHAPTER 1

SEMICONDUCTOR LASER DIODE

1.1 Introduction

The development of semiconductor laser diodes traces its origin to the early 1960s shortly after the invention of other laser systems. These lasers are an innovation that has revolutionized the world we live in. Semiconductor laser diodes are arguably the most important of all lasers due to their wide variety of applications, ranging from readout sources in compact disk players to transmitters in optical fiber communication systems. They are widely used in many experiments in optical and atomic physics. They have well-known features and characteristics like high reliability, miniature size, lower power consumption, wide tunability, high efficiency, and excellent direct modulation capability. Although these devices are compact, simple, and relatively inexpensive, unmodified laser diodes do have some undesirable properties, mostly as a result of their short semiconductor cavity [1].

1.2 Fundamentals of Laser Operation

This thesis work relies heavily on exploiting the properties of a semiconductor laser diode. Before we begin to discuss these properties, it is necessary to understand the basic principles of lasers and conditions necessary for diode laser operation.

1.2.1 Absorption, Spontaneous and Stimulated Emission

We explore the fundamentals of light absorption, spontaneous emission, and stimulated emission in a two-level system in a single atom or molecule with a

monochromatic electromagnetic wave. Any electron in an atom or molecule has its own stable states in which the atom has a specific energy level. When an electron makes a transition from one stationary state to another, the atom radiates energy. The frequency of the light radiation is related to the energies of the states by Bohr's principle

$$\nu = [E_f - E_i]/h, \quad (1.1)$$

where E_f and E_i are energy levels of final and initial states in an atom or molecule and h is Planck's constant.

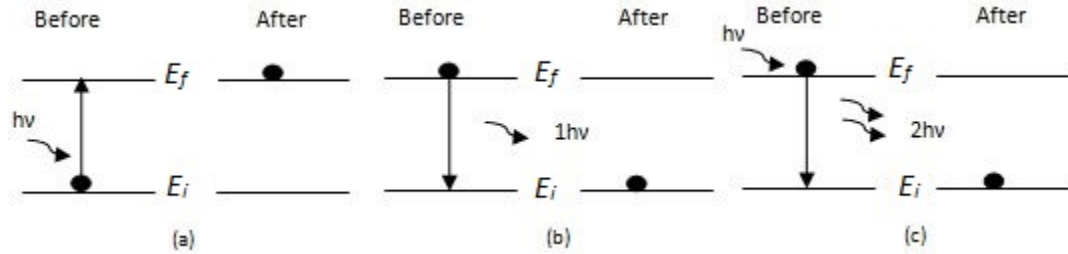


Figure 1.1: Three types of transitions (a) Resonant absorption, (b) Spontaneous emission, (c) Stimulated emission.

There are three different kinds of atomic transitions between two different states due to the interaction of light. The first type of transition of an atom illustrated in Figure 1.1(a) is referred to as resonant absorption. Assume an atom is initially residing in the ground state with energy E_i ; the atom stays in the ground state until a photon of frequency $\nu = \nu_0$ is incident, where ν_0 is the transition frequency between two energy levels. In this case, there is a maximum probability for an atom to make a transition from the lower level E_i to the higher level E_f by absorption of a quanta of light. Figure 1.1(b) represents a process in which an atom in the higher energy level decays to the lower stable level after spending a definite time in the higher level. The corresponding energy difference $E_f - E_i$ must be

released by spontaneously emitting a quanta of light. Since each atom makes a transition independently, a photon is emitted in a random direction with a random phase. Such light is incoherent and the process is defined as spontaneous emission. The third kind of transition shown in Figure 1.1(c) is referred to as stimulated emission. In this case, an atom is initially in the final state, and a light of frequency $\nu = \nu_0$ is incident on an atom or a molecule; the incident photon will cause an atom to undergo a transition from E_f to E_i in such a way that a new photon is generated in addition to the incident photon. The generated photon has the same phase and direction as that of an incident photon and is known as the coherent light.

1.2.2 Population Inversion and Pumping

In order to generate a laser, atoms or molecules must make transitions by stimulated emission. Two conditions must be fulfilled for lasing action to occur. First, more atoms must be in a higher excited state than in lower energy levels, i.e., there must be a population inversion (necessary condition for lasing). This condition is necessary or else the light emitted by stimulated emissions will be re-absorbed by atoms at a rate that is greater than the emission rate. Therefore, external pumping of atoms to higher states is required to accomplish population inversion. The second important condition is that the stimulated emission rate should be higher than the spontaneous emission rates in an active medium (sufficient condition for lasing) [1].

1.2.3 Optical Resonators

An optical resonator is used to feedback new generated coherent light into the medium. The coherent light of a laser is achieved by coupling the active medium with a laser cavity. The cavity selects some of the photons emitted spontaneously to

repropagate through the medium. Neglecting any phase shifts in the cavity, the allowed wavelength is given by

$$\lambda_n = 2L/n, \quad (1.2)$$

where L is the length of a linear laser cavity and n is the harmonic mode of the wave. Thus, the cavity allows only those photons whose wavelength can form a standing wave in the cavity. This limits the wavelength and direction of the photons allowed to repropagate through the medium. These photons induce other photons with the same propagating direction, phase, and wavelength via stimulated emission, and in a brief time all the photons propagating through the cavity are coherent. To get this coherent light out of the cavity and make use of it, one of the reflective ends of the cavity is made semi-reflective, thus, allowing some of the coherent light to escape. The rate at which the photons are randomly absorbed or exit through the semireflective ends of the cavity is called transmission loss. This does not include other losses like absorption or diffraction losses. The rate at which the photons give rise to other photons via stimulated emission is called gain. To have a functioning laser, the gain versus overall loss ratio must be greater than one. Beyond the aforementioned requirement for population inversion, the other two main requirements for laser operation are an active light-emitting medium and an optical resonator for regenerating the radiation field [2].

1.3 Semiconductor Laser Diode

A semiconductor laser diode is a specially fabricated p-n junction device that emits coherent light when it is forward biased. When atoms or molecules come together into a semiconductor crystal, the discrete atomic energy level smears into energy bands, which are significantly different from discrete energy levels, as shown

in Figure 1.2.

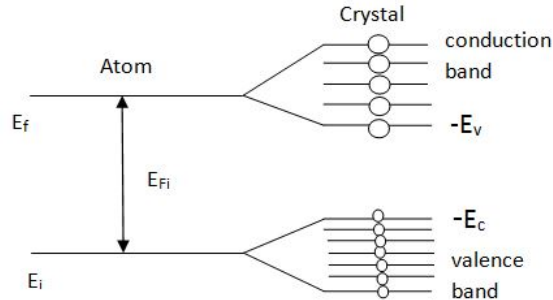


Figure 1.2: Energy level diagram for an atom and a crystal.

The semiconductor valence band is formed by multiple splitting of the highest occupied atomic energy level of the constituent atoms; likewise, the next higher-lying atomic level splits apart into a conduction band [1]. The population inversion in a semiconductor laser diode is produced when a p-doped semiconductor material is joined with an n-doped semiconductor material. The n-doped material contains an excess of electrons and the p-doped material has an excess of holes (a material with excess positive charge). When a voltage is applied across the junction with the positive voltage on the p side, the electrons are pulled through the junction towards the positive electrode, and the holes are attracted to the negative side. This produces an electrical current flow across the junction. The electrons and the holes meet within a junction because of opposite charges. The electron-hole pair meet, recombine, emit radiation, and produce a population inversion. This inversion occurs between energy levels located above and below the semiconductor band gap.

The energy band above the gap is the conduction band and the one below the gap is the valence band. The energy gap typically corresponds to a wavelength near the infrared region (refer to Figure 1.3). Hence, most semiconductors radiate in near

infrared region and are not transparent in the visible spectral region [3]. The optical feedback is implemented by reflections, which are usually implemented by cleaving the semiconductor material along its crystal planes. The refractive index difference between the crystal and the surrounding air causes the cleaved surfaces to act as reflectors. Thus, the semiconductor material acts both as a gain medium and a Fabry-Perot optical resonator [4].

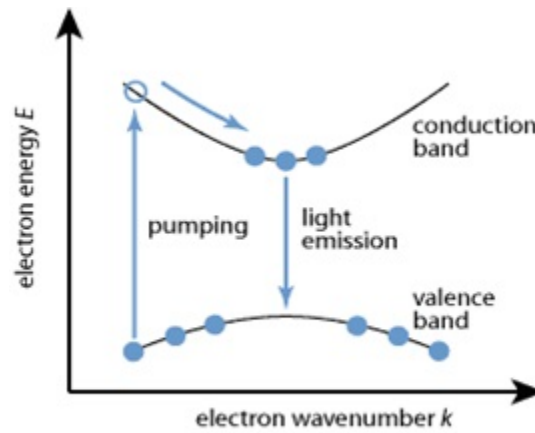


Figure 1.3: Energy bands in semiconductors.

1.4 Basic Characteristics of a Semiconductor Laser Diode

The first continuous wave double heterostructure laser diode operating at room temperature was demonstrated in 1970 by Zhores Alferov. In this section, we consider some elementary properties of laser diode characteristics such as threshold current, output power, beam divergence, and spectral content.

1.4.1 Threshold current and threshold current density

Threshold current is one of the most important basic parameters of laser diodes. It specifies the degree at which they emit light when current is injected into

the devices. As the injected current is increased, the laser first demonstrates spontaneous emission. The spontaneous emission increases very gradually until it begins to emit stimulated radiation, which is the onset of laser action. Threshold current is the exact current value at which this phenomenon takes place. It is generally desirable that the threshold current be as low as possible, resulting in a more efficient device. Thus, a threshold current is one measure used to quantify the performance of a laser diode.

Threshold current is dependent on the quality of the semiconductor material from which the device is fabricated and the general design of the structure of the device waveguide. However, it is also dependent on the size and area of a laser device. One laser diode could demonstrate a much higher threshold current than another device and still be considered a much better laser. This is because the area of the device can be large. A laser that is wider or longer requires more electrical power to reach the onset of laser action than a laser of a smaller area. As a result, when comparing the threshold current values of different devices, it is more appropriate to talk about threshold current density rather than threshold current. Threshold current density is denoted by the symbol J_{th} and is determined by dividing the experimentally obtained threshold current value I_{th} by the cross-sectional area of the laser gain medium. Threshold current density is one of the parameters that is a direct indication of the quality of a semiconductor material from which the device is fabricated. When comparing the performance of various laser devices, one must compare the threshold current density values rather than the threshold current values. While calculating the current density of the laser, it is necessary to accurately measure the area of the laser through which current is being injected [5].

1.4.2 Output Power

Output power is another parameter used to characterize a laser diode.

Figure 1.4 [5] shows an experimental result, which depicts output power of a typical continuous wave (CW) semiconductor diode laser as a function of injection current (L-I curve).

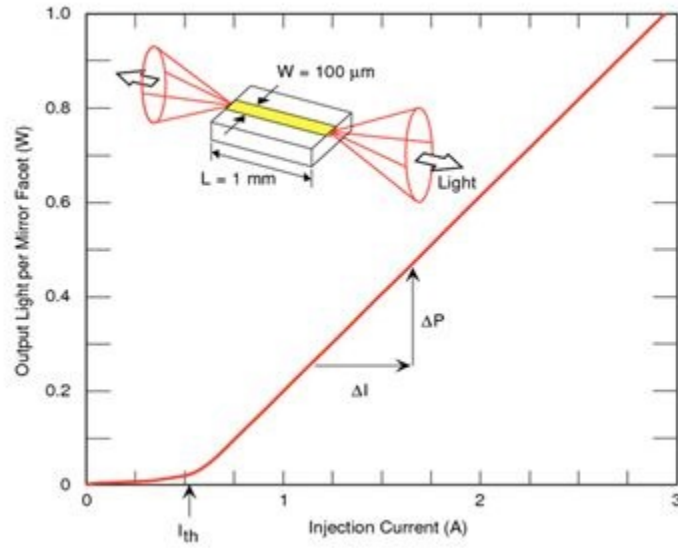


Figure 1.4: Output light versus injection current in a semiconductor diode laser(reprinted with permission from Newport tutorial).

The efficiency of a laser in converting electric power to light power is determined by the slope of the L-I curve, denoted by the change in output power over the change in current ($\Delta P/\Delta I$). The inset in Figure 1.4 schematically shows a broad area ($100 \mu\text{m}$ wide stripe) laser diode emitting radiation from both its front and back mirror facets. When the forward bias current is low, the laser diode operates like light-emitting diodes (LEDs) where the carrier density in the active layer is not high enough for population inversion; spontaneous emission is dominant in this region. As the forward bias current increases, population inversion occurs.

Stimulated emission becomes dominant at a certain bias current as the threshold current. The injection current above the threshold induces the abrupt onset of laser action, and coherent light is emitted from the diode laser. The laser's threshold current is evaluated by extrapolating the linear part of the L-I curve to zero output power. If the injection current is increased to excessively high values, the L-I curve becomes sub-linear. Operation at high current shortens the lifetime and can fatally damage the laser [1].

1.4.3 Beam Divergence and Astigmatism

Divergence of the output laser beam from a diode laser is described in Figure 1.5.

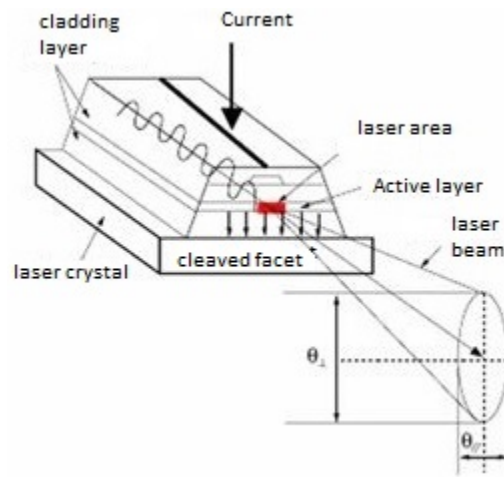


Figure 1.5: Structure and lasing mode in a semiconductor laser.

The beam is diffraction-limited in both planes of the junction (orthogonal and parallel) due to the small size of the laser diode chip. The output of a laser diode is highly divergent, special collimating optics are often used since many applications require collimated light. Either molded spherical or multiple element glass lenses are used to collimate the output. These lenses typically have a numerical aperture of

0.5 or better to collect the entire laser output beam. Using lenses, the output light of a laser diode can be formed into a collimated beam with little divergence. If a gain-guided laser diode beam is collimated or being focused, then a cylindrical lens is used to account for astigmatism. Astigmatism is a condition in which the apparent focal points of the two axis do not coincide. It limits the ability to focus the laser beam into a small spot size and complicates focusing the output beam to a sharp well-defined point. A long focal length lens is used to compensate for the astigmatism and then the collimating lens can provide a beam that has little divergence in both axis [5].

1.4.4 Optical Spectrum

The optical spectrum of a laser diode depends on particular characteristics of the laser's optical cavity.

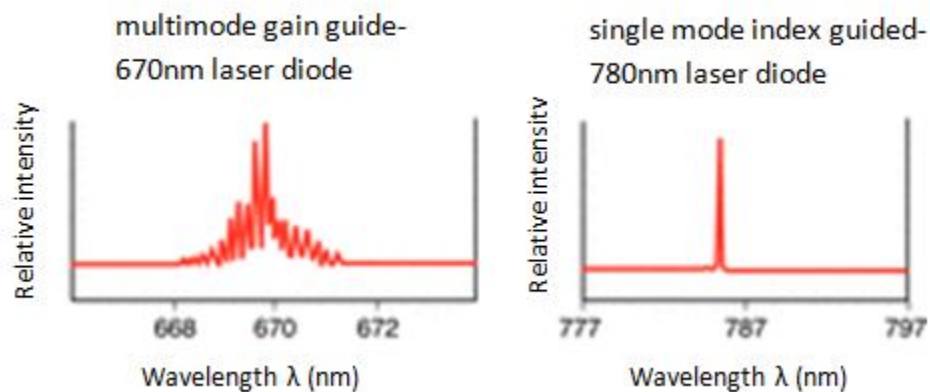


Figure 1.6: Multimode versus single mode spectra (reprinted with permission from Newport tutorial).

Most conventional gain or index-guided devices have a spectrum with multiple peaks, whereas distributed feedback (DFB) and distributed-Bragg-reflector (DBR)

type of devices display a single well-defined spectral peak. Figure 1.6 [5] shows a comparison between these two spectral behaviors. The number of spectral lines that a laser is capable of supporting is a function of the cavity structure, as well as operating current. The result is that the multimode laser diodes exhibit spectral outputs with multiple peaks around their center wavelength.

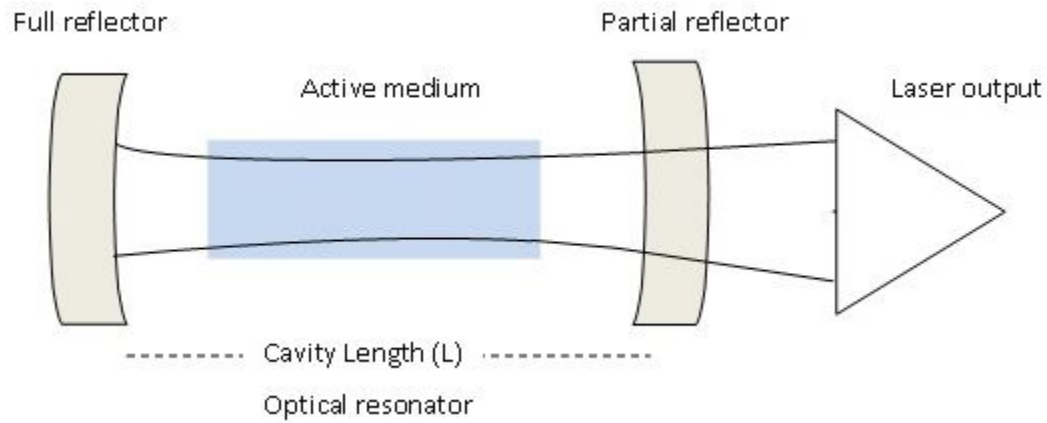


Figure 1.7: Geometry of a linear laser cavity.

The optical wave propagating through the laser cavity forms a standing wave between the two mirror facets of the laser. The distance L between the two mirrors determines the period of oscillation of this curve. This standing optical wave resonates only when the cavity length L is an integer number m of half wavelength existing between the two mirrors. In other words, a node must exist at each end of the cavity. The only way this can take place is for L to be exactly a whole number multiple of half wavelength $\lambda/2$, where λ is the wavelength of light in a semiconductor material and is related to the wavelength of light in free space λ_0 through the index of refraction n by the relationship $\lambda = \lambda_0/n$. As a result of this situation, there can exist many longitudinal modes in the cavity of a laser diode, each resonating at its distinct wavelength of $\lambda_m = 2L/m$. From this, we can note

that two adjacent longitudinal laser modes are separated by a wavelength

$$\Delta\lambda = (\lambda_0)^2/2nL. \quad (1.3)$$

1.4.5 Center Wavelength Change with Temperature

There is a linear relationship between temperature and center wavelength. As temperature increases, the center wavelength of the laser diode also increases. This characteristic is useful in spectroscopy applications, laser diode pumping of solid state lasers, and erbium-doped fiber amplifiers, where the wavelength of emission of the laser diode can be accurately temperature-tuned to the specific properties of the material with which it is interacting [5].

1.4.6 Mode Hopping

The short continuous segments in Figure 1.8 [5] indicate the tuning of the optical length of a cavity for a given longitudinal mode. When the peak of the gain medium has shifted too far, the laser jumps to another mode. This is indicated by the breaks in the curve.

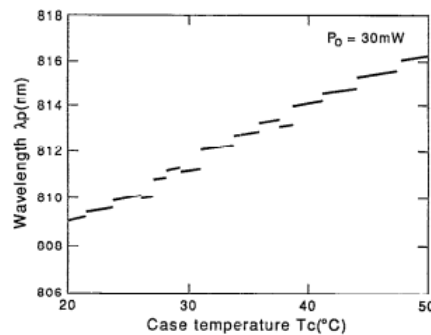


Figure 1.8: Mode hopping observed while temperature tuning a laser diode (reprinted with permission from Newport tutorial).

Single-mode lasers exhibit this phenomenon called mode hopping, in which

the center frequency of the laser diode hops over discrete wavelength bands and does not show continuous tuning over a broad range. One can change the wavelength where the discontinuities take place by making small adjustments to the drive current. When selecting a specific laser diode for an application requiring a specific wavelength such as spectroscopy, mode hopping must be taken into account while temperature tuning the device.

1.5 Types of Semiconductor Diode Laser

There are many types of diode lasers. Each type of diode laser has its own features and by choosing the correct type of diode laser for the given application, the right performance can be obtained. Some of the main types of diode lasers include the following:

1.5.1 Double Heterostructure Diode Laser

The double heterostructure diode laser is made up by sandwiching a layer of a high band-gap material by layers of low band-gap material on either side. This makes the two heterojunctions, as the materials themselves are different and not just the same material with different types of doping. Common materials for the double heterojunction diode laser are gallium arsenide (GaAs), and aluminum gallium arsenide (AlGaAs). The advantage of the double heterojunction diode laser over other types is that the holes and electrons are confined to the thin middle layer which acts as an active region. By containing the electrons and holes within this area more effectively, more electron-hole pairs are available for the laser optical amplification process. Additionally, the change in material at the heterojunction helps contain the light within the active region providing additional benefit.

1.5.2 Quantum Well Diode Laser

The quantum well diode laser uses a very thin middle layer; this acts as a quantum well where the vertical component of the electron wave function is quantized. As the quantum well has an abrupt edge, this concentrates electrons in energy states that contribute to laser action, which increases the efficiency of the system. In addition to the single quantum well lasers, multiple quantum well lasers also exist. The presence of multiple quantum wells improves the overlap of the gain region with the optical waveguide mode.

1.5.3 Quantum Cascade Diode Laser

A quantum cascade diode laser is a form of heterojunction laser in which the difference between well energy levels is used to provide laser light generation. This allows the laser diode to generate relatively long wavelength light. The actual wavelength can be adjusted during fabrication by altering the laser diode layer thickness.

1.5.4 Separate Confinement Heterostructure Diode Laser

This type of diode laser has been widely used for the majority of diode lasers since 1990s. The separate confinement diode laser overcomes the problem that exists in many other forms of diode laser, the thin laser layer is too thin to confine the light effectively. This laser overcomes the problem by adding another two layers with a lower refractive index on the outside of the existing ones. This effectively confines the light to within the diode.

1.5.5 Other Types of Diode Lasers

Distributed feedback diode lasers (DFB), are used in forms of telecommunications or data transmission using optical systems. Here the laser diode wavelength is important, but laser diodes are not particularly stable in this respect with wavelength varying with temperature, voltage, ageing, etc. A diffraction grating is etched close to the p-n junction of the diode to assist in stabilizing the wavelength of the generated light signal. This grating acts like an optical filter causing a single wavelength to be fed back to the gain region. The pitch of the grating is set during manufacture, and it only varies slightly with temperature.

Vertical-cavity surface-emitting diode lasers are a form of surface emitting laser and they emit the laser radiation in a direction perpendicular to the substrate, delivering a few milliwatts with high beam quality [6].

External cavity diode lasers contain a laser diode as the gain medium of a longer free space cavity (extended cavity). These lasers are often wavelength-tunable and they exhibit a small emission spectral linewidth. We characterize and study this type of diode laser in this thesis.

CHAPTER 2

EXTENDED CAVITY DIODE LASER

2.1 Introduction

The first experiment on a laser diode coupled to an external cavity was performed by Crowe and Craig in 1964 [7], soon after the first successful operation of a diode laser. With the development of semiconductor diode lasers, tunable extended cavity diode lasers are finding a wide variety of applications in a broad range of fields. They are of considerable interest in coherent optical telecommunications, atomic and molecular laser spectroscopy, precise measurements, and environmental monitors. An overview of the most important applications is outlined as follows:

- **Optical coherent telecommunications:** Drop-add multiplexers, elimination of wavelength blocking, easy use of optical core.
- **Sensing:** Ultra-high resolution spectroscopy, optical radar, atmospheric and environmental studies, industrial processing monitoring.
- **Precise measurements:** Atomic clock and magnetometer, optical spectrum analysis, device characterization.

In addition to the typical applications exemplified above, there are many other applications, including nonlinear optical conversion, optical data storage, coherent optical transient processing, and quantum optical manipulation and engineering [1]. Tunable diode lasers are widely used in atomic physics. This is primarily because

they are reliable sources of narrow band (< 1 MHz) light and are vastly less expensive than traditional tunable dye or Ti-Sapphire lasers. However, the frequency tuning characteristics of the light from a diode laser are far from ideal, which greatly reduces its utility. In particular, the laser output is some tens of megahertz wide and can be continuously tuned only over certain limited regions. These characteristics can be improved by the use of optical feedback to control the frequency of the laser [8]. There are many possible techniques for the wavelength tuning of semiconductor diode lasers. One of the practical approaches is tunable external cavity diode lasers (ECDLs), that could provide an alternative to monolithic semiconductor diode lasers for accomplishing the wide tuning of a diode laser [1].

2.2 Design of an Extended Cavity Diode Laser

In designing an external cavity diode laser system, a few elementary concerns must be taken into consideration. We need to maximize the feedback, to precisely align the laser cavity, to select the wavelength, and to accurately control the laser chip temperature and extract the excess heat [9]. A tunable external cavity diode laser system consists primarily of a semiconductor diode laser with or without antireflection coatings on one or two facets, a collimator for coupling the output of the diode laser, and an external mode-selection filter. In general, the features of a diode laser in an external cavity can change greatly depending on the length of the external cavity, feedback strength, optical power, and diode laser parameters. Littman-Metcalf configuration and Littrow cavity configuration (Figure 2.1) are typical examples of ECDL sources in which gratings are used to provide optical feedback, select single-mode operation, and tune the wavelength over the whole

range of gain bandwidth by changing the grating position and orientation [1].

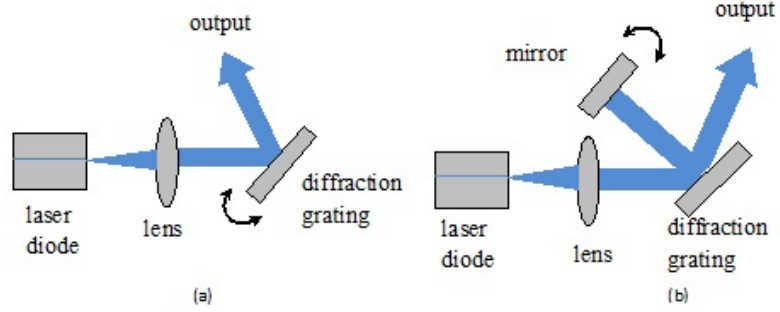


Figure 2.1: Tunable external cavity diode laser with (a) Littrow and (b) Littman configuration.

2.2.1 Littrow Cavity Configuration

The frequency of the tunable laser diode is very sensitive to changes in temperature and injection current, and has large linewidths (~ 100 MHz) and poor tunability. It is well known that these shortcomings can be rectified by operating the laser in a longer external cavity which provides frequency-selective optical feedback. A particularly simple implementation of this idea uses feedback from a diffraction grating mounted in a Littrow configuration (refer to Figure 2.2).

In a Littrow configuration, first-order light which is diffracted from a grating is coupled back into the laser diode, and the directly reflected light forms the output beam [10]. The formula for constructively diffracted orders of light reflected from a diffraction grating is:

$$d \sin \theta = m\lambda, \quad (2.1)$$

where d is the spacing between the grooves, θ is the angle of incidence, λ is the wavelength of the incident light, and m is an integer. One consequence of the above equation is that spectra diffracted off a grating are reproduced at several different

angular positions about the grating [2].

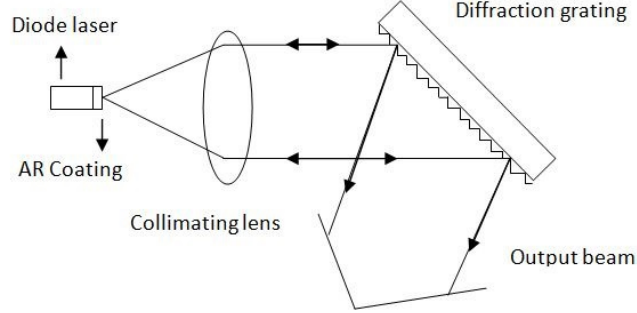


Figure 2.2: Littrow configuration set up.

The various replications of the spectra are called orders of diffraction and obey the grating equation:

$$(\sin \theta_i + \sin \theta_m) = m\lambda/d, \quad (2.2)$$

where θ_m is the angle of the m^{th} order diffracted beam, θ_i , m and λ are incident angle, an integer, and wavelength. The Littrow angle (when $\theta_m = -\theta_i$) is determined from the grating equation 2.2. If we define θ_L as the angle of incidence, then the equation for the Littrow angle of the system becomes:

$$2d \sin \theta_L = m\lambda. \quad (2.3)$$

This particularly simple and effective configuration can be used with a blazed grating to reduce feedback and increase output power, thus improving overall efficiency. This configuration is analogous to the addition of standing waves on an oscillating rope. Littrow configuration is made possible with the implementation of blazed gratings (refer to Figure 2.3).

Blazing is a technique of shaping individual grooves of a diffraction grating so that the diffraction envelope maximum shifts into another order. While the

diffraction envelope is shifted by the shaping of the individual grooves, the interference maxima remains fixed in position. Their positions are determined by the grating equation(2.2), in which angles are measured relative to the plane of the grating. The result is that the diffraction maxima now favor a principal maximum of higher order ($|m|>0$) and the grating redirects the bulk of the energy in that particular order [11].

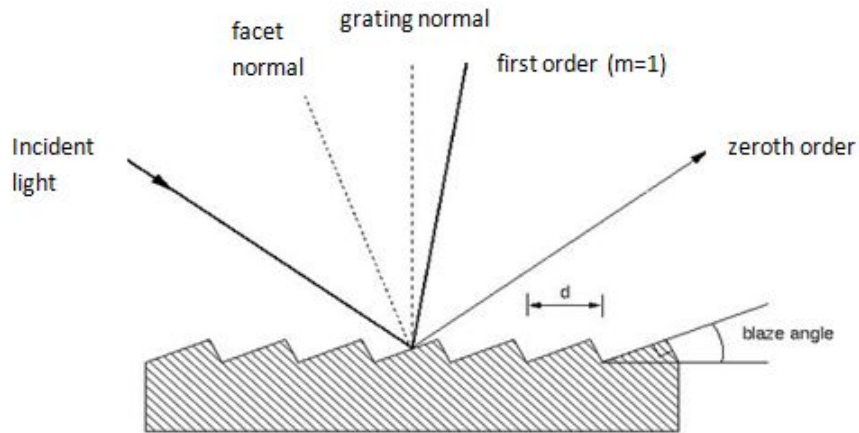


Figure 2.3: Blazed grating.

2.3 Components and Parts of an ECDL

We have built an extended cavity diode laser of the design mentioned by Arnold, Boshier and Wilson [10], [8]. It is an effective method with inexpensive components that helps in reducing the linewidth and improving the wavelength tunability of a diode laser. This design has three basic components, a commercial diode laser, a diffraction grating, and a collimating lens. These components are mounted on a base plate. The laser and lens are mounted in such a way that the lens can be carefully positioned relative to the laser to ensure proper collimation.

The diffraction grating is mounted in the Littrow configuration. The emission wavelength can be tuned by rotating the diffraction grating. The grating serves as one end mirror of the laser cavity with the back facet of the diode providing the second mirror. In order to tune the frequency of the laser, we must change the length of the cavity in a properly controlled manner. This can be done by a piezo electric transducer stack/disk (Thorlab model- AE0203D04F) attached to the grating that moves the grating in response to applied voltage.

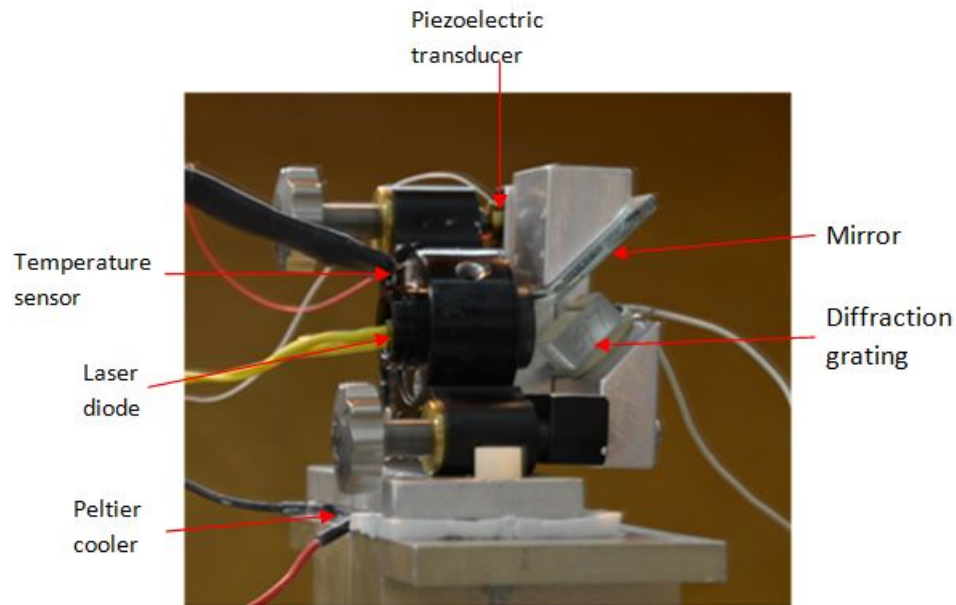


Figure 2.4: Extended Cavity Diode Laser (ECDL) set up.

Figure 2.4 displays our experimental setup of an ECDL. Our design uses various low cost commercial components. We have used a Sanyo DL7140 201S infrared laser diode emitting light of wavelength 785nm (typically). A collimation tube (Thorlab) holds the laser diode and the collimating lens. The optical output of the laser diode is very divergent with a beam divergence of 7° (FWHM) in parallel and 17° (FWHM) in perpendicular directions, so we need to use a lens close to the

laser facet to collimate the output. We also use a Thorlab holographic diffraction grating GH13-12V with 1200 lines per mm. Most of the light is directly reflected by the grating ($m=0$ order), but roughly 20% is reflected back into the laser ($m=1$ order). The grating forms an external cavity (i.e., external to the laser's own internal semiconductor cavity), which serves to frequency-stabilize and line-narrow the laser output. With the simple addition of a diffraction grating, the laser is now less sensitive to stray light feedback, and its linewidth is reduced to $\Delta\nu < 1$ MHz, much smaller than the atomic transition linewidths we will be observing.

The injection current necessary to run the laser is provided by the low noise current driver (Thorlab LDC 1100). A thermoelectric Peltier cooler (TEC) maintains the laser diode at a set temperature by actively cooling or heating the entire mechanical setup. In order to ensure that the entire laser setup is at the same temperature, all laser components have been polished to have maximum surface contact between them. We also use heat-conducting thermal paste to optimize thermal conductivity. The TEC is driven by a proportional-integral-derivative controller (PID controller-model-XMT 700). It is a generic control loop feedback mechanism widely used in industrial control systems. The PID temperature controller stabilizes the temperature of a laser to the set temperature within approximately 0.5° Celsius. The TEC is sandwiched between two conductive aluminum plates at the base of the laser mount and is coupled to a thermistor Pt100 (a Platinum100 resistor whose resistance varies with temperature). The thermistor buried inside the laser mount (not visible in Figure 2.4), serves as a laser temperature sensor for the PID controller. The entire laser setup is mounted on an aluminum block which serves as a large heat sink. The block is mounted stably on an optical table, providing vibrational and mechanical stability, dampening and an additional heat sink.

2.4 Operating Principle of an ECDL

To operate an extended cavity diode laser, we connect the laser diode with the laser diode current controller (LDC) by checking the polarities of the current driver and the laser diode. We slowly increase the current in the diode until lasing is observed (sudden increase in the brightness of the output as viewed by a fluorescent card used to visualize the presence of IR radiation). The power builds up in a laser diode and above threshold, the power increases proportionally to the difference between the current and the threshold value (Figure 1.4). Above threshold, there is adequate population inversion such that stimulated emission is dominant. When ramping the diode, we take caution and do not change the current too abruptly, for the laser is very sensitive to surges or transient currents. We are also careful not to exceed the laser diode's maximum operating current i.e., 100 mA [12].

The output laser beam is elongated and divergent. We rotate the collimation tube in the laser mount until the long axis of the beam is horizontal. The laser is linearly polarized along the long axis of the facet and the laser output is roughly Gaussian. The laser output is collimated by adjusting the position of the lens with a wrench i.e., the lens is on a threaded mount that can have its position adjusted by rotating the lens holder. The laser diode should be exactly one focal length away from the collimating lens. In practice, the best way to see if the laser is at the focal point of the lens is to remove the back half of the ECDL, which is the diffraction grating and mount, and aim the entire laser housing at a distant wall. Now we see if the size of the output beam on the wall is of the same size as that observed when shining the laser on a piece of paper placed right in front of the setup. It is possible for us to have an agreement in the size of the light beam on the wall and that of the beam on the piece of paper and still have the output not collimated. Therefore, we

examine the spread of the laser beam on the piece of paper, when the paper is at several different points between the laser diode and the wall. If the size of the spread is constant regardless of the position of the paper, then the laser is collimated. Aside from being collimated, it is also desirable to have the output from the laser level with the horizontal plane. The laser beam must be horizontal so that the first order diffracted beam will be directed back at the collimating lens rather than above or below it [2].

2.5 Alignment of an ECDL

The following methods are used to align the grating with respect to the laser output, such that the Littrow condition stated before can be satisfied. Due to the fact that the aperture of the lasing chip is 0.1 mm by 0.3 mm, physically positioning the grating based on simple geometry is not practical [12]. Therefore, we employ a pin-hole method followed by a current scanning method to align the grating and check for optical feedback.

First, we stabilize the temperature of the laser diode mount at 66° Fahrenheit. As illustrated in Figure 2.5, the output light from the laser diode is incident on the grating, and the diffracted light gets reflected from the mirror, M2, attached parallel to the grating. The beam 1 coming out from the optical set up is made to retro-reflect from an external mirror, M1, placed in front of the mount. This is checked by a small piece of paper (with a pin hole) placed in front of the laser beam coming out of the mount. If the reflected spot from the external mirror is seen above or below the pin hole, we adjust the alignment of the external mirror, M1, until the laser beam is retroreflected (beam 2), so the reflected spot coincides with the pinhole (incident beam). Then, we adjust the orientation of the grating with the

help of vertical and horizontal actuators (not shown in Figure 2.5) so that the light (beam 3) sent back into the optical set-up is retroreflected back towards the pinhole and passes through it a third time. Injecting light back into the laser from the grating gives rise to a buildup of light at a frequency determined by the external cavity, leading to preferential lasing on this mode and concomitantly a reduction in the laser threshold. Observing the change in the laser threshold therefore provides another way to align the grating using the current scanning technique.

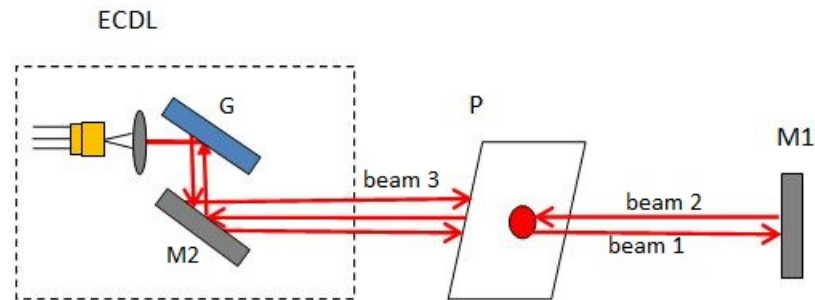


Figure 2.5: Pin hole alignment technique, G: grating, P: piece of paper with a pin hole, M2: mirror attached inside the mount parallel to the grating, M1: external mirror, LD: laser diode.

In the current scanning technique, we monitor the laser output using a power meter or a photodiode. After crudely aligning the grating, we operate the laser at a current close to threshold. Then we modulate the laser current with a saw tooth waveform from the frequency generator (10 Hz). If the laser power is then monitored on a photodiode and displayed on an oscilloscope in X-Y mode (refer to Figure 2.6 showing the detected power as a function of the current level), we get a real time monitor of the laser threshold (i.e., the knee in power that is recorded when measuring the output power versus current for the bare diode). Alignment of the grating then shifts the position of this knee and the optimum injection is found,

when the threshold is again reduced to a minimum (the knee is furthest to the left on the oscilloscope). Finally, when the grating is satisfactorily well injected, we record the power versus current curve again around threshold, in order to determine the new threshold current. This will form a future reference point that will allow us to determine whether the laser is still well injected. Note also that the horizontal alignment is the most critical, as generally the laser will inject over a range of wavelengths (equivalently grating angles or vertical positions), but in the horizontal direction there is only one correct alignment [13].

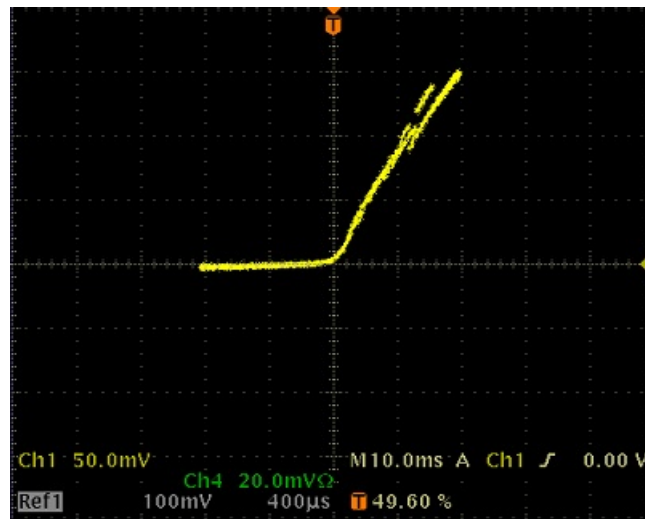


Figure 2.6: L-I curve.

2.6 Calibration of an ECDL: Mode-Hop Suppression

Mode-hop suppression in a tunable laser with a Littrow configuration feedback cavity can be obtained in terms of simultaneously sweeping the Littrow grating angle and the external-cavity length. The simplest way to obtain such coupled movements is to rotate the Littrow grating about a particular axis. It has been shown that there is an optimal point which provides the maximum continuous

tuning range [14]. This concept is discussed later on in detail with Figure 2.8. It is possible to tune a laser wavelength in a wide range of 240 nm near 1450 nm with an external cavity diode laser with mode-hops [15]. However, a continuous tuning range of 15 nm around 1300 nm without mode hop has been achieved with the same type of ECDLs and a simple mechanical arrangement [16].

In such lasers, the grating angle controls the wavelength λ_r associated with minimum losses. Nevertheless, the lasing wavelength also depends on the cavity length that determine resonant mode positions. Continuous tuning is obtained if the resonant wavelength λ_q of the longitudinal mode number q and the minimum loss wavelength λ_r are spectrally shifted at the same rate to keep the lasing mode in a low-loss region. This condition can be fulfilled by the use of a rotation-translation combination of the grating positions. Despite the complex mechanical setup and stability requirements, we can tune a single-mode laser by moving the grating. To understand how the laser frequency changes when the grating is moved, we have to examine several cases [17].

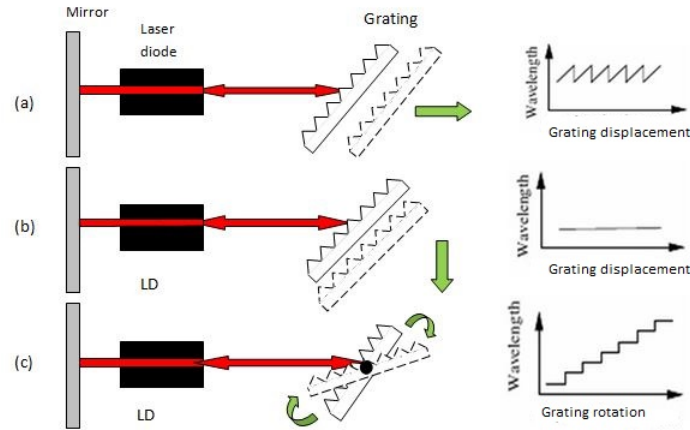


Figure 2.7: Different ways to move the grating and the corresponding change in wavelength.

In Figure 2.7(a), the grating is moved along the laser beam direction, the standing wave oscillating inside the cavity will be stretched, resulting in a continuous tuning of frequency. But as the frequency changes, this stretching also varies the diffraction angle from the grating. After a while, a mode with one more half-wave period inside the cavity will point directly towards the mirror; i.e., the mode will have low losses, leading to an abrupt mode hop back in frequency as shown in the right side of Figure 2.7(a). If, however, the grating is moved perpendicular to the beam, as illustrated in Figure 2.7(b), the distance between any particular groove on the grating and the mirror does not change. This means that even though the cavity is becoming longer, there is no change in the frequency of the light diffracted back in to the laser. We can also vary the frequency of the laser by changing the angle of the grating, thereby, choosing the frequency feedback to the laser. If the grating is turned around the center point of the beam, as shown in Figure 2.7(c), the frequency of the cavity at the middle of the beam will not change. This means that there is no variation of frequency until the next possible mode has lower losses, and then the laser mode hops to the new frequency. In order to achieve continuous tuning with no mode hops, the grating has to be translated and rotated in a coordinated way. It is possible to use grating rotation only to optimize the exact position of the rotation axis and to obtain optimum continuous wavelength tuning.

In Figure 2.8, the intersection of the laser axis and the grating plane is denoted by G. The origin of the axis is at point O, $OG=L$, where L is the optical length of the laser cavity. The first order diffraction of the grating is reflected back to the cavity at a grating angle θ . For a grating period d , λ_r is given by:

$$\lambda_r = 2d \sin \theta. \quad (2.4)$$

Taking into consideration the grating translation in its plane, the resonant cavity

mode wavelength λ_q (refer to equation 1.2) is given by a well known equation:

$$\lambda_q = 2L/q, \quad (2.5)$$

It is assumed that the grating is rotated about a point R in such a way that the mode frequency λ_q is exactly at the minimum-loss frequency λ_r . So equating 2.4 and 2.5 gives:

$$\sin \theta = L/qd. \quad (2.6)$$

From Figure 2.8, we get $\sin \theta = L/P$. Therefore, the condition for mode-hop suppression is satisfied if the distance $P = qd$. In other words, the optimum rotation point that provides continuous tuning is the point R as indicated in Figure 2.8.

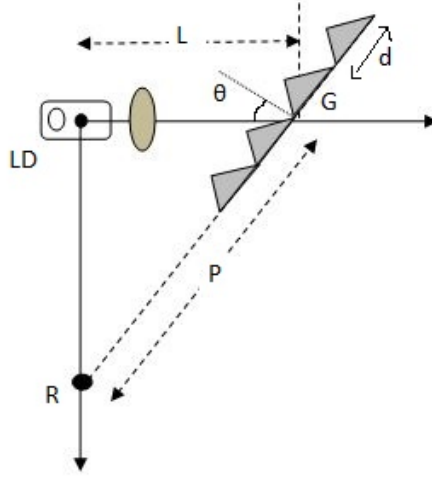


Figure 2.8: Schematic diagram of laser configuration showing optimum rotation point R, LD: laser diode, G: grating.

CHAPTER 3

FREQUENCY TUNING PARAMETERS OF THE ECDL

3.1 Introduction

The tuning parameters presented in this chapter control the frequency output of our laser. At the level of precision that we need for our experiment, the laser is not adequately stabilized. So we are continuously adjusting these tuning parameters so that the laser frequency does not deviate from a stable reference frequency (atomic spectrum).

3.2 First Tuning Parameter- Temperature

Thermal expansion changes the cavity length of a semiconductor chip in a laser diode. An increase in temperature increases the cavity length and so the resonant wavelength. It also shifts the semiconductor gain peak towards longer wavelengths (shorter frequencies). The laser frequency can be changed by changing the temperature of the laser. The temperature of a laser diode may be adjusted externally. We can vary the temperature from 0°C to 40°C, and a typical temperature tuning is 0.03 nm/°C, or 15GHz/°C. The advantage of using this tuning parameter is that large changes in frequency are possible. However, there are some disadvantages. First, it can take up to half an hour for the temperature of the laser to stabilize completely. Second, it is very difficult to make small changes in laser frequency, so the tuning that can be achieved is very coarse [18].

3.3 Second Tuning Parameter- Injection Current

The injection current alters the temperature of a laser through Joule heating: $P_{LD}=IR^2\sim mc\Delta T$, where R is the effective resistance of the lasing chip, I is the injection current, m and c are effective mass and specific heat capacity of the laser diode. Altering the injection current is a simple way of indirectly changing the temperature. The injection current also increases the carrier density within the lasing medium, which affects the refractive index. However, once the injection current reaches the threshold, carrier density is clamped and the injection current has command of the laser through temperature only. Unlike direct temperature control, which is usually accomplished externally, injection current raises the laser temperature internally and thus elicits a much faster response from the laser. A typical frequency tuning rate for the injection current is approximately 4 GHz/mA. The injection current is a tuning parameter that shifts both the lasing cavity modes and the gain profile simultaneously, and at different rates, producing a staircase mode hopping tuning curve mentioned in chapter 1 (refer to Figure 1.8). The power output of the laser depends linearly on the injection current beyond the threshold current. The power is given by:

$$P_0 = n_{ex}(h\nu/e)(I - I_{th}), \quad (3.1)$$

where n_{ex} is the differential external quantum efficiency which is equal to the flux per unit change of current above threshold and I_{th} is the threshold current value. In this way the injection current not only changes the laser diode temperature but also changes the output power. The power versus current curve is an important characteristic of a laser and should be among the primary measurements made. It should also be noted that the entire power versus current curve is shifted by a constant amount as the temperature is altered, such that: $I_{th}(T)$ is proportional to

$\exp(T/T_0)$, where T_0 is the characteristic temperature of the laser diode material. The curve shifts by about 0.4 mA/ $^{\circ}$ C for a typical diode laser [12].

3.4 Third Tuning Parameter- Grating Optical Feedback

The light emitted by the laser diode strikes a grating. The grating reflects a narrow frequency range back into the laser, forcing the laser to emit light within that particular frequency range. By changing the angle of the grating with respect to the incoming light, different frequencies may be sent back into the laser, making it possible to tune the laser to a particular frequency range. The grating is mounted on a custom made aluminum piece which is attached to the modified movable commercial mount displayed in Figure 2.4. The movable commercial mount is attached to the fixed laser mount, but it can be rotated. Adjustable screws are used to coarsely adjust the grating angle by pushing on the modified mount.

Fine adjustment is achieved by a piezoelectric transducer (PZT) which is sandwiched between the laser mount and the modified mount holding the grating. The PZT stack, made up of ceramic material, expands in response to an applied DC voltage (as high as 150V) provided by a PZT driver. The expansion of the PZT is proportional to the applied voltage. Voltage applied to the PZT changes its thickness, thereby causing the modified mount to move, changing the angle of the grating relative to the laser light. Figure 3.1 displays the working of the PZT which is placed behind the grating.

Depending on the voltage on the piezo element, the angle ϕ changes, thereby changing the wavelength. As with laser current, this tuning parameter allows for fine frequency adjustment. For every volt that is applied to the PZT by the PZT driver, the frequency of the laser can be changed. This tuning parameter also elicits

a faster laser response than the thermo-electric cooler [18].

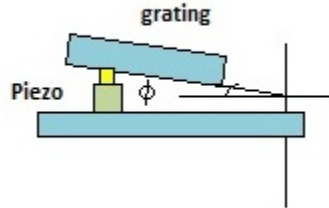


Figure 3.1: Tuning the wavelength with the grating.

3.5 Data Collection and Analysis

In our set up, a Mach Zehnder interferometer with mismatched arm lengths is used to determine the frequency drift of the diode laser with the change in the injection current and PZT voltage.

3.5.1 Mach Zehnder Interferometer

The Mach Zehnder interferometer was developed by physicists Ludwig Mach and Ludwig Zehnder. It uses two separate beam splitters (BS) to split and recombine the beams and give two output beams, which can be sent to photodetectors. The optical path length in the two arms may be identical or different (i.e., with an extra delay line). The distribution of optical power at the two outputs depends on the precise difference in optical arm lengths and on the wavelength (optical frequency) of the beam. If the interferometer is well aligned, the path length difference can be adjusted (i.e., by slightly moving one of the mirrors) so that for a particular optical frequency, the total power goes into one of the outputs. For misaligned beams (i.e., with one mirror being slightly tilted), there will

be some fringe patterns in both outputs, and variations of the path length difference affect mainly the shape of these interference patterns, whereas the distribution of total power on the outputs may not change very much [19].

We are using a Mach Zehnder interferometer with arm lengths mismatched to determine the change in the frequency of the ECDL with tuning parameters (current and PZT). The set up of the Mach-Zehnder interferometer is shown in Figure 3.2.

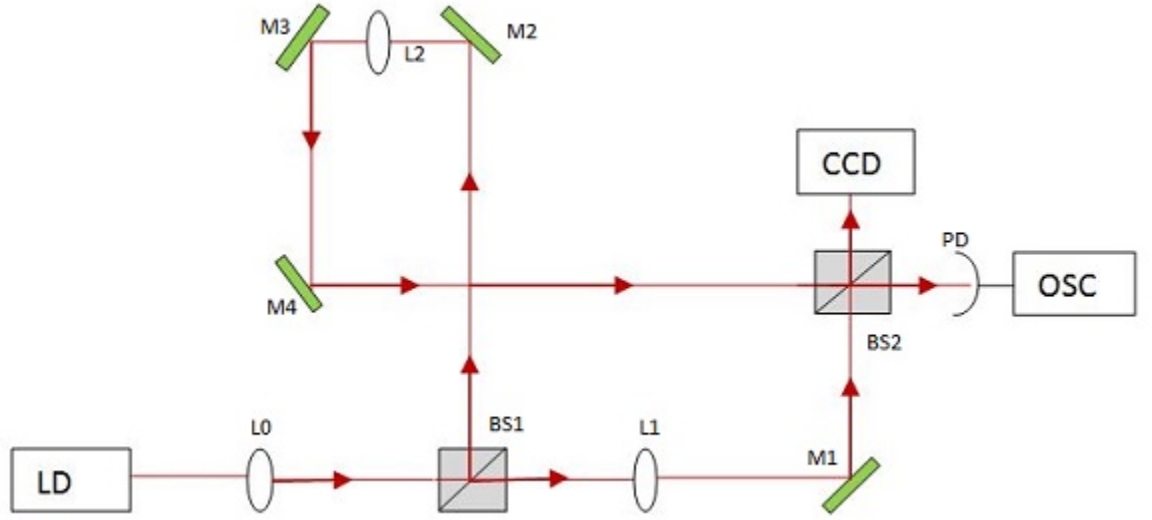


Figure 3.2: Mach Zehnder interferometer set up, LD-laser diode, BS-beam splitter, L-Lens, M-mirror, PD-photodiode, OSC-oscilloscope, CCD-Camera.

The light beam from the laser diode is divided into two beams by the beam splitter BS1. One beam goes to mirror M2 and after reflecting from mirrors M3 and M4, it reaches beam splitter BS2. The other beam gets reflected by mirror M1. The two beams recombine at the beam splitter, BS2 after travelling distances $D1$ and $D2$. Here the distance $D1$ is 80 cm and $D2$ is 4 m. The lenses, L1 of focal length 20 cm and L2 of focal length 100 cm, are placed midway between the two interfering beam paths. They are used for proper mode matching of the beams. Another lens

L0 of focal length 25 cm is placed between the laser and the beam splitter BS1. The two interfering beams will have phase difference (due to the path difference) given by:

$$\phi_1 - \phi_2 = 2\pi(D2 - D1)/\lambda = \nu 2\pi(D2 - D1)/c, \quad (3.2)$$

Here ν is the laser frequency and $(D2 - D1)$ is the path difference between the two beams. The frequency of the laser is not fixed, rather it is swept by the triangular waveform applied to the laser diode current controller. Hence as the laser frequency changes, the phase difference will change. The changes in frequency and phase are expressed by writing the equation given above as:

$$\Delta(\phi_1 - \phi_2) = 2\pi(\Delta\nu)(D2 - D1)/c. \quad (3.3)$$

The intensity of the two superimposed waves, aside from a constant of proportionality, is given by $I = EE^*$

$$I = (E_1 e^{2i\pi(D1/\lambda - \nu/t)} + E_2 e^{2i\pi(D2/\lambda - \nu/t)})(E_1 e^{2i\pi(D1/\lambda - \nu/t)} + E_2 e^{2i\pi(D2/\lambda - \nu/t)})^* \quad (3.4)$$

or $I = |E_1|^2 + |E_2|^2 + 2E_1 E_2 \cos[\Delta(\phi_1 - \phi_2)]$, where Δ is inserted to indicate the change in phase from sweeping the frequency. The interference is maximum, whenever:

$$\Delta(\phi_1 - \phi_2) = 2n\pi. \quad (3.5)$$

where n is an integer, substituting Eq. (3.5) into (3.3) yields the frequency spacing of the interference maxima given by:

$$\Delta\nu = c/(D2 - D1), \quad (3.6)$$

here $c = 3 \times 10^8$ m/s and $(D2 - D1) = 3.2$ m; after solving we get $\Delta\nu = 93.7$ MHz.

There are a few factors to consider in order to get good fringes from the interferometer. First, we should not be misled by weak fringes obtained from

interference of the beams reflecting off the two sides of the beam splitter as they will not have the correct spacing. Second, we need to realize that in order to get good fringes, the two beams must not only overlap at the photodiode, but they must also be parallel. The larger the angle between the beams, the closer will be the spacing of the fringes. As we adjust the beams to be parallel (but still overlapping), the spacing between the dark fringes will become larger until it is as large as the photodiode, and we see a large modulation in the photodiode output by changing the frequency. Often the easiest way to get good fringes is to first make the beams as parallel and overlapping as possible. Then we make the final adjustments by looking at the photodiode output and aligning the beams to get the largest fringes as we ramp the laser frequency [19].

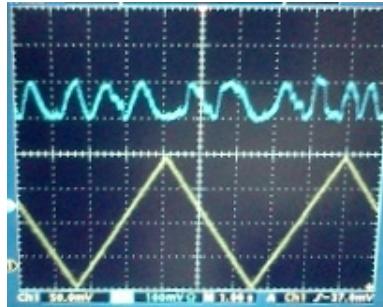


Figure 3.3: Mach Zehnder interference pattern showing frequency change with PZT voltage, the top blue signal shows interference fringes and the bottom one is PZT voltage.

Figure 3.3 is a photograph of the oscilloscope screen showing the triangle waveform and the interference pattern, where the frequency spacing between the maxima is given by Eq. (3.6). Now we determine how large a frequency change is produced for each volt that is applied to the piezo drive and the injection current. As the laser frequency is changed, we observe a cosine modulation on the oscilloscope.

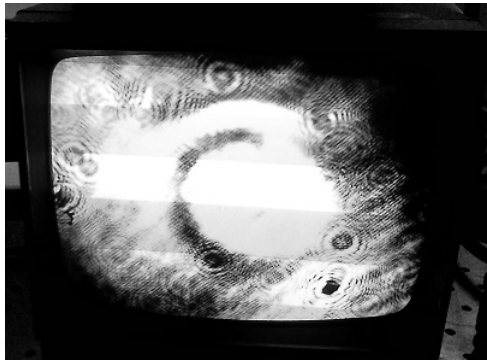


Figure 3.4: Mach Zehnder interference pattern seen through a CCD camera.

According to Eq.(3.4), we observe the change in intensity of the interference pattern due to variation in current and PZT voltage. By counting the number of fringes in a half-waveform as measured on the oscilloscope and multiplying this number by $\Delta\nu$, we will get the total frequency shift per unit volt. However, if we make a large sweep, we see sudden jumps in the signal as if the phase has abruptly changed. What has actually happened is that the laser has jumped to a different frequency (so called “mode hop” as was discussed in the chapter 1). The frequency where the laser jumps will move, if we change the laser current. Under ideal conditions, with this laser setup, we can get a scan of about 8 GHz without a mode-hop. More typically we can get continuous scans (no mode hops) of 3 or 4 GHz. If the frequency range over which we get a continuous scan is shorter than this, it probably means that the vertical alignment is off. The length of continuous scan can also be affected by the laser temperature. We also used a CCD camera to observe the interference pattern. Figure 3.4 displays the interference pattern through the CCD. Table 3.1 and 3.2 shows the data that we collected.

Table 3.1: Frequency drift versus injection current.

LDC current (mA)	No. of fringes in 7 mA amplitude waveform	Total frequency shift (GHz/Volt)
36	25	15.6
46	28	17.5
56	26	16.2
66	27	16.9
76	25	15.6
86	16	10
96	23	14.4

Table 3.2: Frequency drift versus PZT Voltage.

PZT Stack Voltage (Volt)	No. of fringes in 1 Volt amplitude waveform	Total frequency shift (GHz/Volt)
3	13	0.223
15	16	0.100
22	14	0.058
35	15	0.040
42	16	0.035
56	14	0.023
69	13	0.017
74	13	0.016
85	11	0.012
92	12	0.012

CHAPTER 4

ATOMIC SPECTROSCOPY- RUBIDIUM CELL

4.1 Introduction

Atomic transitions can offer a good frequency reference over a wide wavelength range and a stable frequency reference under various environmental conditions like fluctuating temperature, varying pressure, and strain. Transitions between hyperfine energy levels of the alkali atom rubidium are used as a frequency reference in our experiment.

4.2 Basic Concept of Frequency Stabilization

The output frequency of an external cavity diode laser depends upon injection current and temperature. To obtain a stable frequency output, it is important to stabilize the diode's temperature and injection current. In a laser diode with Littrow configuration, the optical feedback from the grating is spectrally narrowed and peaked at a frequency that can differ from the central frequency of the free-running diode laser. The feedback narrows the laser linewidth from 50 MHz to less than 1 MHz. The central frequency will be very close to that of the feedback signal. Many experiments require a laser with a well-defined frequency. But over time, the central frequency of a diode laser with grating feedback will drift; this drift is caused by fluctuations in temperature, injection current, and mechanical conditions. Stabilizing the laser by locking it to an external reference reduces this drift. Laser frequency stabilization is based on the generation of a frequency error signal, which passes through zero at the locking frequency. To achieve the frequency

stabilization of a diode laser, a portion of the output diode laser beam is compared with a frequency reference, an error signal is generated which is then converted into an electrical signal and feedback to a diode laser after amplification if necessary[18].

There are a variety of reference frequencies which can be used to stabilize the frequency of a diode laser. In order to stabilize the frequency of our laser, we need a highly stable optical reference frequency. The hyperfine atomic transitions of the rubidium-85 isotope provides the level of stability that we need. We use a technique known as saturated absorption spectroscopy to produce a spectrum of narrow peaks to which we can lock the frequency of the laser by means of the feedback circuit. These peaks correspond to different hyperfine transitions of Rb_{85} . By carefully adjusting the laser temperature, injection current, and grating angle as described in Chapter 3, we can tune our laser to one of these hyperfine atomic transitions. Our optical setup is divided into two main parts: a laser frequency monitoring section and a Doppler-free or saturated absorption spectroscopy apparatus.

4.3 Monitoring the Laser Frequency

After the grating is aligned and the injection is optimized, it is unlikely that our laser operates at a wavelength coincident with an atomic transition. Tuning the wavelength so that the laser is on transition requires adjustment of the vertical actuator together with the laser current and temperature. We direct some or the entire laser output beam through an atomic vapor cell and observe the cell with an infrared viewer. We expect to see the fluorescence when the laser is resonant with an atomic transition [13]. If we fail to tune through an atomic resonance, we employ an optical spectrum analyzer (model MS9001B/B1) that will reveal the absolute operating wavelength (nominally 780 nm) of the laser output directly to about +/-

0.1nm. Although the wavemeter conveniently displays the output wavelength, this convenience comes at the cost of coupling the output laser light into a multi-mode optical fiber cable which is then connected to the input of the wavemeter. The wavemeter is a scanning Michelson interferometer that measures interference fringes of the input light, and compares them to a reference. We now have a functioning laser tuned to an atomic transition and is ready for some atomic spectroscopy.

4.4 Rubidium Vapor Cell

The Rb vapor cell is a glass cell filled with natural rubidium having two isotopes: Rb_{85} and Rb_{87} . The vapor pressure of rubidium inside the cell is determined by the cell temperature and is about 4×10^{-5} Pa at room temperature. It is the frequency standard to which the diode laser frequency is compared. In the 780 nm range, there are 4 absorption lines each separated by approximately 8 GHz. The lines in the Rb are Doppler broadened. The follow up experiment will involve Doppler broadened and Doppler free spectrum of the Rb atoms. The width of the Doppler broadened profile is approximately 500 MHz.

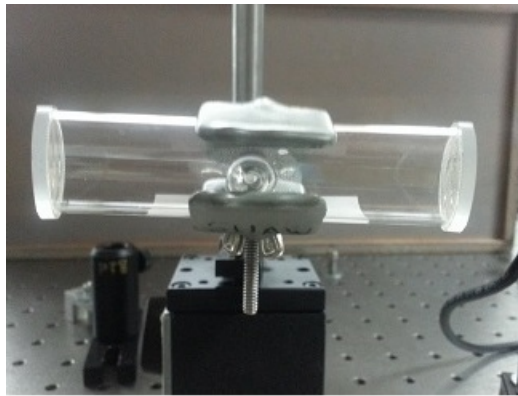


Figure 4.1: Rubidium vapor cell.

The rubidium atom (Rb) has an atomic number 37. In its lowest configuration

(ground state), it has one electron outside an inert gas core (Argon) and is described by the notation $1s^2 2s^2 2p^6 3s^2 3p^6 3d^{10} 4s^2 4p^6 5s$. The integers 1 through 5 above specify principal quantum numbers 'n'. The letters s, p, and d specify orbital angular momentum quantum numbers 'l' as 0, 1, and 2, respectively. The superscript indicates the number of electrons with the values of n and l. Rb ground state configuration is said to have filled shells up to the 4p orbital and a single valence (or optical) electron in a 5s orbital. The next higher energy configuration has the 5s valence electron promoted to a 5p orbital with no change to the description of the remaining 36 electrons.

4.4.1 Fine Structure Levels

Within a configuration, there can be several fine structure energy levels differing in the energy associated with the coulomb and spin-orbit interactions. The coulomb interaction is associated with the normal electrostatic potential energy kq_1q_2/r_{12} between each pair of electrons and between each electron and the nucleus. where k is coulomb's constant, q_1, q_2 are the magnitude of charges, and r_{12} is the vector distance between the charges. (Most, but not all of the coulomb interaction energy is included in the configuration energy.) The spin-orbit interaction is associated with the orientation energy $(-\vec{\mu} \cdot \vec{B})$ of the magnetic dipole moment μ of each electron in the internal magnetic field B of the atom. The form and strength of these two interactions in rubidium are such that the energy levels are most accurately described in the L-S or Russell-Saunders coupling scheme. L-S coupling introduces new angular momentum quantum numbers L, S, and J as described next.

- L is the quantum number describing the magnitude of the total orbital angular momentum L, which is the sum of the orbital angular momentum of

each electron:

$$L = \sum l_i \quad (4.1)$$

- S is the quantum number describing the magnitude of the total electronic spin angular momentum S, which is the sum of the spin angular momentum of each electron:

$$S = \sum s_i \quad (4.2)$$

- J is the quantum number describing the magnitude of the total electronic angular momentum J, which is the sum of the total orbital and total spin angular momentum:

$$J = L + S \quad (4.3)$$

The values for L, S and J are specified in a notation $^{(2S+1)}L_J$ invented by early spectroscopists. The letters S, P, and D (as with the letters s, p, and d for individual electrons) are used for L and corresponds to L = 0, 1, and 2, respectively. The value of (2S + 1) is called the multiplicity and is thus 1 for S = 0 and called a singlet, 2 for S = 1/2 (doublet), 3 for S = 1 (triplet), etc. The value of J (with allowed values from |L - S| to |L + S|) is annotated as a subscript to the value of L.

The sum of l_i or s_i over all electrons in any filled orbital is always zero. Thus for Rb configurations with only one valence electron, there is only one allowed value for L and S: the value of l_i and s_i for that electron. In its ground state (5s) configuration, Rb is described by L = 0 and S = 1/2. The only possible value for J is then 1/2 and the fine structure state would be labeled $^2S_{1/2}$. Its next higher (5p) configuration is described by L=1 and S=1/2. In this configuration there are two allowed values of J: 1/2 and 3/2 and these two fine structure states are labeled as $^2P_{1/2}$ and $^2P_{3/2}$ [20].

4.4.2 Hyperfine Levels

Within each fine structure level there can be an even finer set of hyperfine levels differing in the orientation energy (again, a $-\vec{\mu} \cdot \vec{B}$ type energy) associated with the nuclear magnetic moment in the magnetic field of the atom. The nuclear magnetic moment is much smaller than the electron magnetic moment and this is why the hyperfine splitting is so small. The nuclear magnetic moment is proportional to the spin angular momentum I of the nucleus, whose magnitude is described by the quantum number I . Allowed values for I depend on nuclear structure and vary with the isotope. The hyperfine energy levels depend on the total angular momentum F of the atom: the sum of the total electron angular momentum J and the nuclear spin angular momentum I :

$$F = J + I \quad (4.4)$$

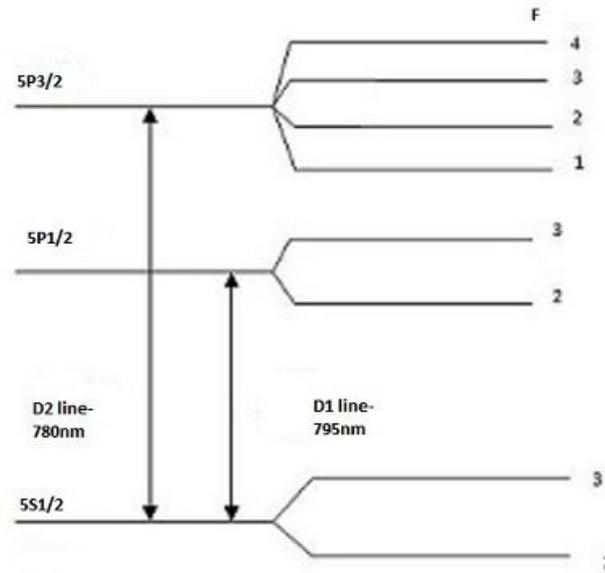


Figure 4.2: Energy manifold of rubidium D2 transition.

The magnitude of F is characterized by the quantum number F with allowed

values from $|J - I|$ to $|J + I|$. There are two naturally occurring isotopes of Rb: 72% abundant Rb_{87} with $I = 3/2$ and 28% abundant Rb_{85} with $I = 5/2$. For both isotopes, this leads to two hyperfine levels within the $^2\text{S}_{1/2}$ and $^2\text{P}_{1/2}$ fine structure levels ($F = I - 1/2$ and $F = I + 1/2$) and four hyperfine levels within the $^2\text{P}_{3/2}$ fine structure level ($F = I - 3/2, I - 1/2, I + 1/2, I + 3/2$) [13]. Figure 4.2 shows the configuration (fine-hyperfine energy strfucture) of the Rb atom.

4.4.3 Transitions

The $^2\text{S}_{1/2}$ to $^2\text{P}_{1/2}$ transitions are all around 795 nm, while the $^2\text{S}_{1/2}$ to $^2\text{P}_{3/2}$ transitions are around 780 nm. We will only discuss the 780 nm transitions that can be reached with the laser used in this experiment. These transitions are displayed in Figure 4.2 [20].

4.5 Doppler Broadened Absorption Spectra

Since the rubidium atoms in the cell are in a gaseous phase, they are in constant motion because of their thermal energy. These atoms are characterized by different velocity classes according to the magnitude of their speed and direction of motion. The zero velocity class, in particular, refers to those atoms that are not moving. When the laser frequency is on resonance with the atomic transition frequency of Rb_{85} , some of the laser light is absorbed by the atoms. As a result, the photodiodes detect less light from the probe beams. By scanning the frequency of our laser across the atomic transition frequency of Rb_{85} , it produces an absorption spectrum. Figure 4.3 displays our optical set up.

Figure 4.4 displays the Doppler-broadened absorption spectrum that we obtained by scanning across the atomic reference frequency. As shown in Figure 4.4, the peaks in the first waveform are due to the flourescence produced by the Rb cell

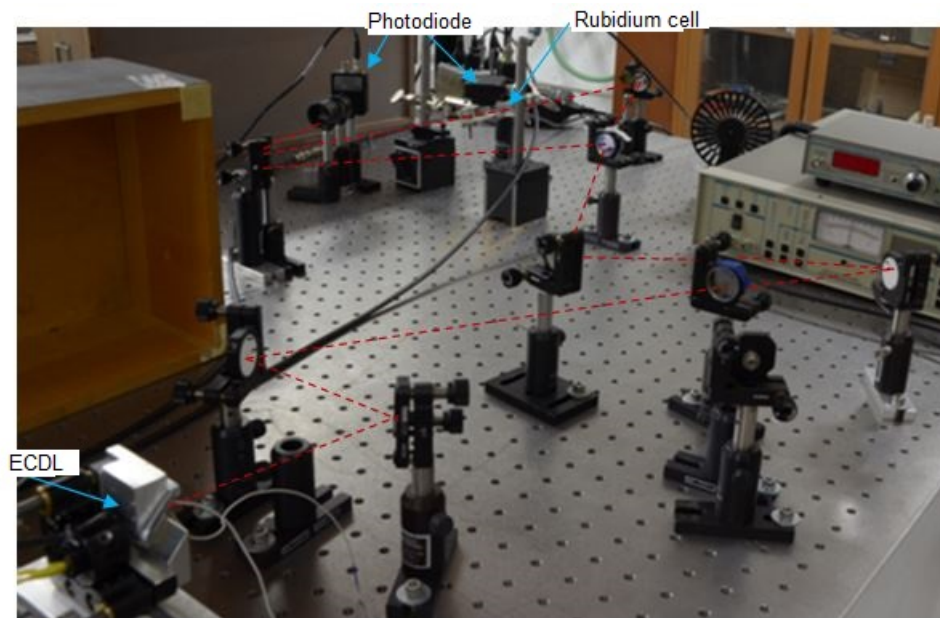


Figure 4.3: Experimental set up of rubidium spectroscopy.

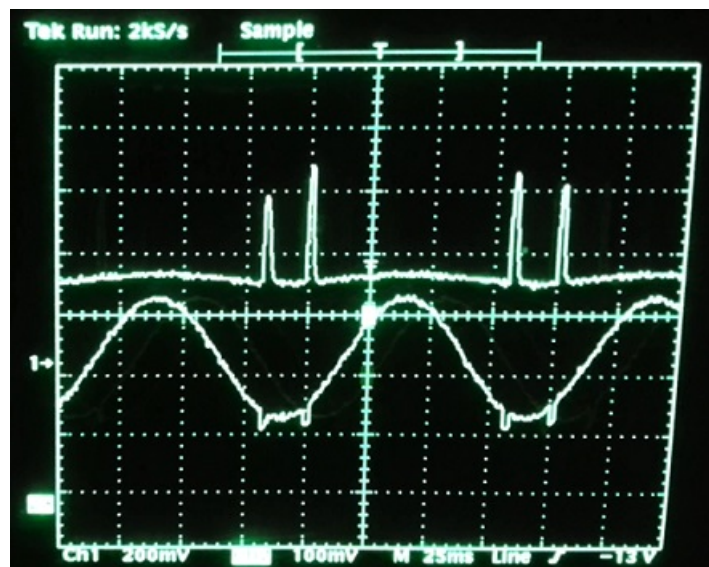


Figure 4.4: Doppler broadened rubidium absorption spectrum.

(the photodiode is placed close to the cell), whereas the second waveform is due to the intensity of the beam transmitting through the cell (the photodiode is placed at the end to the cell).

Intuitively, this spectrum should consist of narrow dips which correspond to the hyperfine transition frequencies of Rb_{85} . However, these dips are broadened due to a phenomenon called Doppler-broadening. Doppler-broadening results from the motion of the atoms with respect to the direction of the laser beam. If an atom is traveling towards the beam, the laser frequency seen by the atom is greater than if it were stationary. As a result, if the laser frequency is slightly lower than that of the atomic transition frequency of Rb_{85} , the Doppler effect would make it seem as if it were on resonance with the transition. This corresponds to the lower frequencies of the Doppler broadened absorption spectrum. A similar effect is observed in the case in which an atom is traveling away from the light beam. The apparent frequency is lower. As a result, light of slightly higher frequency is absorbed. This corresponds to the higher frequencies of the Doppler broadened absorption spectrum. The zero velocity class of atoms does not contribute to Doppler broadening. These atoms, in fact, correspond to the center of the absorption peak and, therefore, a transition frequency [18].

4.6 Saturated Absorption Spectroscopy

One of the popular methods of stabilizing the diode laser is saturated absorption spectroscopy. A narrow peak in a saturated absorption spectrum is often used as an external reference for frequency locking a diode laser. As displayed in Figure 4.5, the main laser beam is split into an intense saturating beam (pump beam) and a weaker probe beam which pass through a rubidium cell in opposite

directions. The saturating beam is strong enough to reduce significantly the population of state capable of absorbing the laser wavelength. The beam bleaches a path through the gas. The probe beam therefore encounters a smaller absorption and registers a higher intensity at the detector. The two beams can interact in this way, however, only when they are both absorbed by the same atoms in the gas and that can happen only when they are both tuned to the wavelength of atoms that have no Doppler shift. In other words, once the pump beam excites a certain atom, it is removed from the pool of excitable atoms available to the probe beam. And once the two beams are overlapped, the absorption of the probe beam is reduced by a factor governed by the number of zero velocity atoms that are excited by the pump beam. As a result, the signal reported by the overlapping probe beam tuned to the lab frame transition reveals Doppler broadened peaks with small dips (called Lamb dips) corresponding to the absorption frequencies of the zero velocity class of atoms only. Since the un-broadened absorption profile is a direct result of the natural linewidth of the atomic transitions, which have a Lorentzian lineshape, these Lamb dips inherit the very same Lorentzian lineshape [12]. In practice, the saturating beam is interrupted by a mechanical chopper and enhancement in the transmission of the probe beam is detected by tuning a laser by a range of wavelengths and searching for a signal at a chopper frequency [21]. Figure 4.6 displays the Lamb dip and the Doppler free absorption spectrum that we obtained.

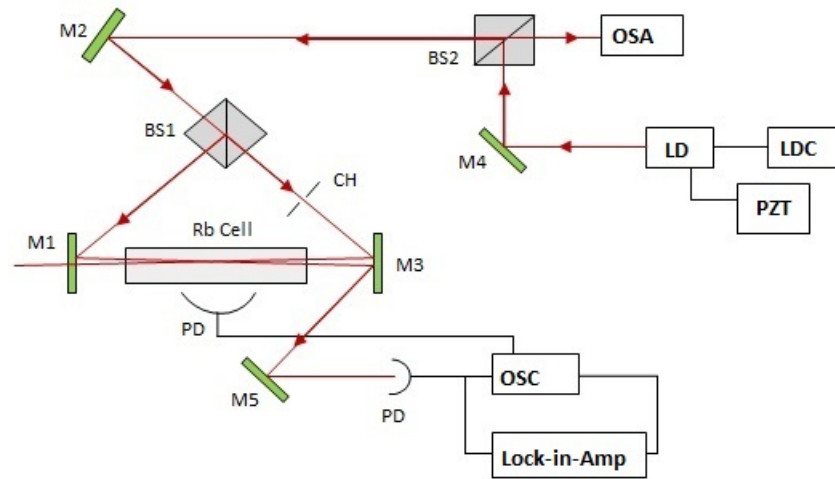


Figure 4.5: Optical set up for rubidium saturated spectroscopy: LD-laser diode, LDC-laser diode controller, PZT- piezoelectric transducer, CH- chopper, M-mirror, BS-beam splitter, PD-photodiode, OSC- oscilloscope, OSA-optical spectrum analyser, Rb cell-rubidium cell, lock-in-Amp-Lock in Amplifier.

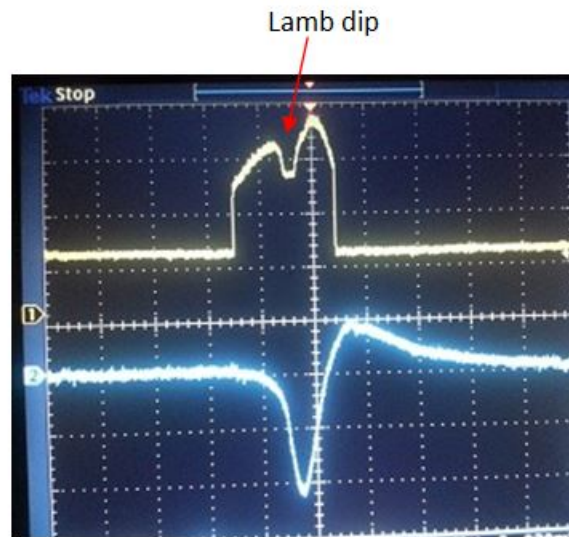


Figure 4.6: Doppler free rubidium absorption spectrum, the top yellow trace shows a dip in the absorption spectral line and the bottom blue trace is the amplified signal from the lock-in amplifier.

CHAPTER 5

ELECTRONIC LOCKING CIRCUIT

5.1 Introduction

Locking a laser means keeping its frequency fixed to an external reference (which may not always be a fixed frequency). The noise spectrum of the laser's frequency fluctuations leads to an effective line-width of the laser, which conceptually describes the broadening of the laser's spectrum around its central frequency [22]. If the laser is locked, the line-width can be reduced and the drift over time is suppressed. The laser is locked to one of the resonance peaks of rubidium absorption spectrum by employing the locking electronics.

Radio-frequency modulation is used to derive an error signal that measures the deviation in frequency to the reference. The error signal is filtered (using the locking electronics) and fed back to the laser. This feedback signal pushes the laser frequency towards the reference point. The phase of the feedback signal is an important parameter. The phase must be less than 180° to push the laser frequency towards the direction of the reference. When the phase is changed by 180° , the frequency will shift in the wrong direction and the laser will be pushed away from the reference [23]. If one succeeds in making the electronic feedback bandwidth (i.e., range of frequencies over which corrections are effectively imposed) wider than the dominant noise spectrum of the laser, the laser's frequency fluctuations can be controlled and the laser can be tightly locked to the reference frequency [22].

5.2 Generating an Error Signal

The first step in the locking procedure is to generate an electronic error signal that can be further processed for locking the laser. We have used a frequency modulation technique to create an error signal. This technique enables detection of the error signal at a high frequency, where the technical noise is near the shot-noise limit. The resulting demodulated error signal has a high signal-to-noise ratio and a large acquisition range, which can produce robust locks. Furthermore, this error signal has odd symmetry about the line center that enables locking at the top of an absorption peak [22].

5.2.1 Frequency Modulation

The laser frequency can be modulated by modulating the injection current of the laser. Our laser diode current controller (LDC 1100) has an analog modulation input which allows the output current to be modulated up to 1 MHz. To achieve higher frequency modulation, directly injecting RF current into the laser diode can be used. In anode injection, the cathode is grounded to the chassis and the RF signal is injected to the anode through a resistor and a capacitor. The inductor L must be present to isolate the power rail which is low impedance to ground the chassis through a capacitor. The circuit and values of the resistor, capacitor and inductor used in the process of RF signal modulation are shown in Figure 5.1.

The laser frequency ω_L is modulated by a modulation frequency f that tunes ω_L periodically from ω_L to $\omega_L + \Delta\omega_L$; therefore, the laser frequency is given by

$$\omega_L(t) = \omega_0 + A \sin(2\pi ft). \quad (5.1)$$

In this equation, ω_0 is the center frequency of an absorption line and A is the amplitude, which corresponds with $\Delta\omega_L$.

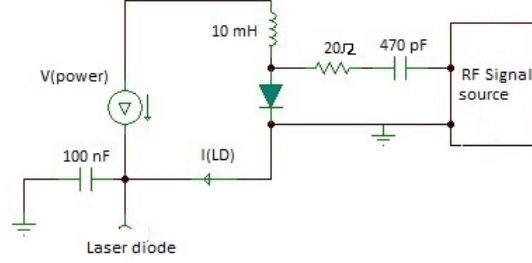


Figure 5.1: RF signal injection to the laser diode current controller.

When the laser is tuned through the absorption spectrum, the difference in the transmitted intensities $[I_T(\omega_L + \Delta\omega_L) - I_T(\omega_L)]$ can be detected by a lock-in amplifier (phase-sensitive detector tuned at the modulation frequency). When the modulation sweep $\omega_L + \Delta\omega_L$ is small enough, it results in the first derivative of the absorption spectrum. This is shown in Figure 5.2. The created signal goes exactly through zero at ω_0 , which makes it a suitable error signal to lock the laser to this center frequency [23]. The basic set-up for this technique is shown in Figure 5.3.

There are several competing factors to consider when choosing the frequency modulation technique. The frequency needs to be sufficiently high, so that the process of filtering and demodulating to base-band does not yield a significant phase shift within the desired feedback bandwidth. We found that choosing a modulation frequency in an order of magnitude higher than the required bandwidth is more than sufficient. Although modulating at even higher frequencies (hundreds of megahertz) is possible, this requires more skills to avoid distorting the DC baseline because of RF pickup. It also makes the local-oscillator phase more susceptible to variations through changes in temperature of the cables, and to residual amplitude modulation (AM) offset errors associated with variations in the optical path length.

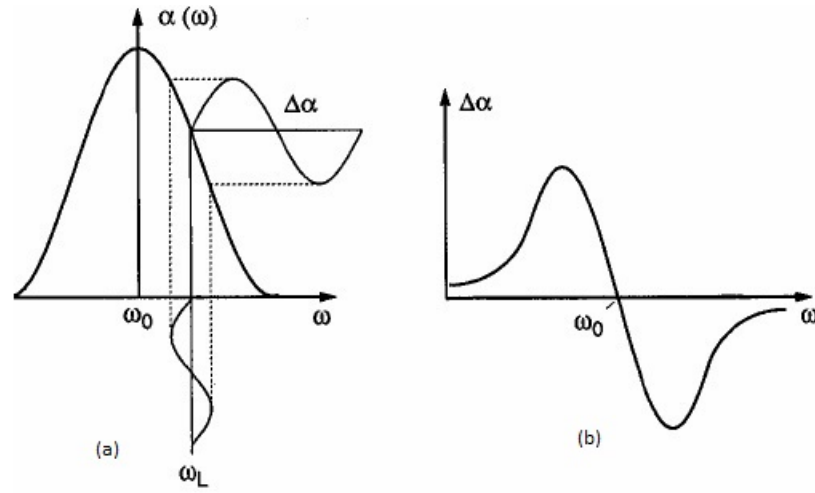


Figure 5.2: Error signal using frequency modulation, (a) power versus frequency plot showing an absorption line, (b) shape of an error signal.

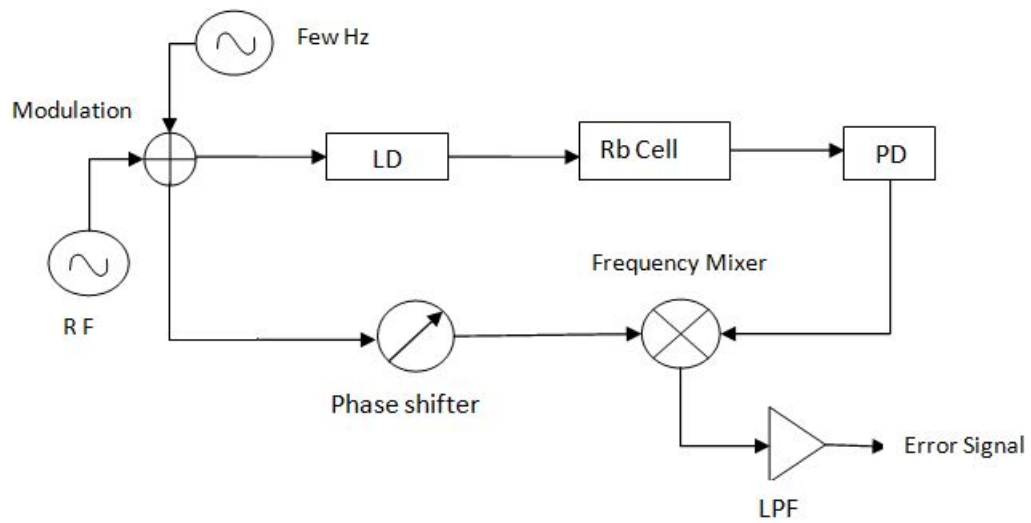


Figure 5.3: Set up for generating an error signal, LD: laser diode, PD: photodiode, Rb cell: rubidium cell, RF: radio-frequency, LPF: Low pass filter.

In practice, we expect that modulation frequencies ranging from 15 MHz to 40 MHz work well. We are using 15 MHz modulation frequency in our set up. The current modulation signal is generated by an RF oscillator and added to the injection current at the output of the current controller (Thorlab LDC 1100) through the circuit mentioned in Figure 5.1. The modulation frequency and modulation amplitude are adjustable by this RF frequency generator.

5.2.2 Demodulation

Once a satisfactory signal is obtained from the detector, it is time to demodulate the error signal so that it will be ready to be used in the servo system. The effect of frequency modulation is to encode the laser frequency fluctuations around the modulation frequency (rather than DC) and then we will decode this error information by mixing it down to DC. The demodulation is easily accomplished by combining the error signal from the detector with a phase-shifted version of the local-oscillator signal used to generate the modulation in a doubly balanced mixer. The phase of the RF local oscillator input to the mixer is adjusted to give a symmetrical frequency discriminator at the mixer output. In the absence of residual amplitude modulation or RF pickup, the center of the resonance will correspond to zero at the output. The error signal must be properly filtered and amplified to control the laser [22].

5.3 Design of the Electronic Feedback Circuit

In this section, we have followed the method and feedback circuit given by Fox et al. [22]. We have build an electronic circuit, in order to create a suitable feedback signal out of the error signal for locking the laser. Our locking electronic circuit consists of two parts, a proportional amplifier and an integrator. The proportional

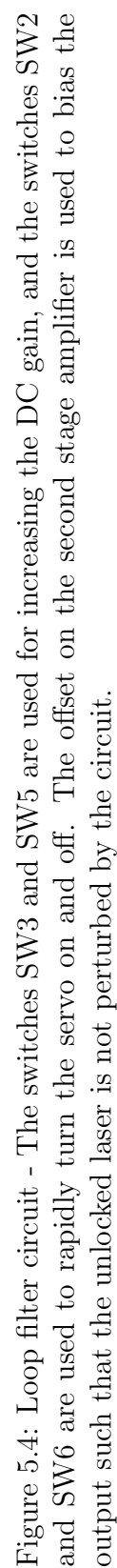
part adds the right offset and gain to the feedback signal. A higher gain makes it lock tightly, but when the gain at high frequencies is too high, it can cause oscillations. The integrator integrates the error signal over a certain time interval to really lock the laser (while getting the error signal to 0). In this locking circuit, the error signal is fed to two paths, piezo and current, with different properties. Different combinations of the resistors and capacitors (passive components) are designed and tested to optimise the gain, phase, bandwidth and to reduce the noise on both paths of the locking circuit [23].

Figure 5.4 displays the final design of our feedback circuit which is built on a printed circuit board (PCB). It includes an error signal circuit as well as electronics for scanning the laser with piezo and current. It is designed using operational amplifiers (opamps) and filters to provide appropriate gain and phase. We can also adjust the shape of the actual loop to approach the desired form by changing the values of various circuit components.

5.3.1 Feedback Loop Filter

The loop filter connects the error signal to the laser, thus completing the feedback loop. The goal of the feedback electronics is to supply enough gain to drive the laser's frequency fluctuations to the noise floor over as much of the servo bandwidth as possible. With proper design, the electronics should neither limit the residual frequency noise level when the laser is locked, nor limit the maximum servo bandwidth. The residual frequency noise should be limited by the light's amplitude fluctuations (technical or shot noise), and the correction speed of the loop should be limited primarily by the laser chip itself. In this section we describe the construction of a loop filter design suitable for locking the frequency of our diode laser.

The task of the servo design is to ensure that there is a sufficient gain at low



Fourier frequencies, while keeping the unity-gain frequency low enough such that the loop is stable. This naturally leads to a gain versus frequency dependence plot with a negative slope. In fact, a plot of this dependence is a standard part of the servo designer's toolbox. These plots called Bode plots are drawn with log-log axes to simplify the interpretation of the various shapes. An example of such a plot is shown in Figure 5.5. A simple picture of the open loop transfer function is the gain as a function of frequency that a signal would experience if it were injected into the diode laser and detected after it travels through the whole system. The bandwidth of the loop refers to the frequency at which the gain falls to 1 (or 0 dB). This is commonly called the unity-gain point, and is often in the range of several megahertz for a servo controlling a diode laser via the injection current. A rule-of-thumb is that at the unity-gain point, the slope of the loop transfer function may not decrease by much more than 20dB per decade of frequency, which corresponds to a factor of 10 per decade or the slope is -1 on the log-log plot. This is necessary to keep the system stable by avoiding positive feedback.

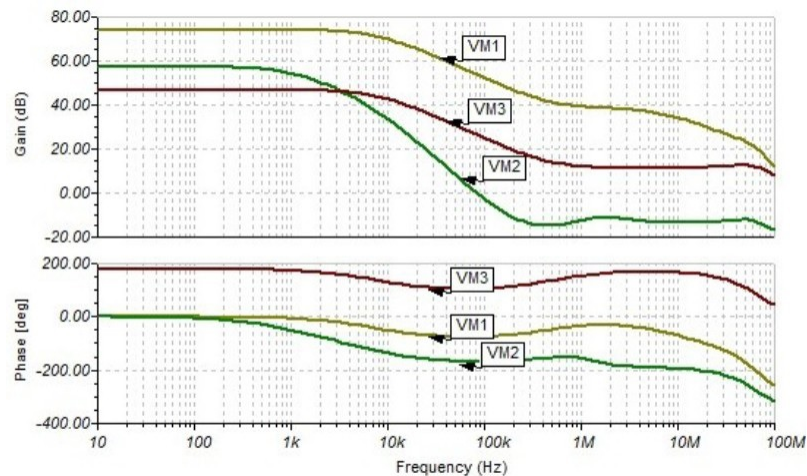


Figure 5.5: Bode plot for the feedback loop filter circuit.

At lower frequencies the slope may be steeper as shown in Figure 5.5, but the transition from a steeper slope to the f^{-1} slope may not occur near the unity-gain frequency. This model transfer function, or Bode Plot, shows loop gain as a function of frequency. Transitions to a steeper slope are caused by RC roll-off elements.

This transfer function fulfills the requirements discussed earlier, namely, large gain at low frequencies while maintaining sufficient phase margin at unity gain to protect against loop oscillations. The three curves shown in Figure 5.5 corresponds to the bode plot at the three junction points of the circuit (refer to Figure 5.4). These plots are generated by simulations of our feedback circuit in the Tina - Ti software [24].

5.3.2 Loop Filter Electronics

The loop transfer function described in the previous section is realized by building a proper electronic loop-filter circuit. Fortunately, a fairly simple circuit based on op-amp electronics is sufficient to provide the gain and shaping required for locking a diode laser. The circuit diagram of the loop filter for our test laser is shown schematically in Figure 5.4. The basic feedback circuit consists of a first stage op-amp that filters and amplifies the error signal coming from the mixer. The output from the first stage is split into two channels, a fast channel that goes to the laser's injection current, and a slower channel that goes to the PZT controlling the length of the extended cavity. The circuit also contains resistors and capacitors which are used to shape the transfer function and control the overall gain. Six switches (controlled manually) are also used to enhance the performance of the servo system.

Let us consider this circuit in more details. We have used a low noise, high speed operational amplifier (OPA355) with unity gain bandwidth of 450 MHz. The

open loop gain of the OPA355 is 100 db. With the initial assumption that all the switches are closed, the first stage consists of an op-amp with parallel RC feedback channels. At DC, the effective opamp gain is above 40 dB, but at the frequency $1/(2\pi RC)$ or 8KHz, the gain starts decreasing and falls as f^{-1} . A much smaller resistor R3 is included in series with the input capacitor C2 in order to limit the very high frequency gain. An extra boost in low-frequency gain (below Fourier frequencies of 8 kHz) can be achieved by opening switch SW3 because then the op-amp functions as an integrator. In fact, the gain at lower frequencies increases as f^{-1} until the amplifier open-loop gain is achieved. Because of the increased gain at low frequencies, opening the integrator switch SW3 forces the error signal even closer to zero. However, with SW3 open, if the laser is not locked to the reference frequency, then amplifier U1 will integrate to a voltage supply rail and locking will not necessarily occur. With SW3 closed, the gain is moderate and the system can respond if the laser frequency is tuned near a reference mode. Therefore, a good strategy is to acquire the locked condition with SW3 closed and then open it after the lock is established.

For Fourier frequencies under 1 KHz, the PZT channel gain becomes significant and is in fact dominant near DC. Another feature of the first stage is the external offset current that is fed in via switch SW1. The op-amp itself should be balanced using the standard offset compensation circuit, but we have chosen to include an additional offset current channel because the circuit is used with injection current modulation. In this case, substantial current offsets are necessary to compensate for the laser's amplitude modulation.

The output from the first-stage amplifier is then sent through separate paths to the two correction elements. First let us consider the fast path, which passes through a variable attenuator and goes to op-amp U2 that feeds current to the laser

diode. If gain beyond that provided by the first stage is needed, one can appropriately set the feedback resistance on op-amp U2. The resulting fast correction signal is sent to the diode laser through switch SW6 and a 2 k Ω resistor. This resistance together with any capacitance inherent in the laser will form a low-pass filter, possibly contributing phase lag that would affect the system bandwidth. In order to provide phase-lead to compensate the diode laser, we have added parallel capacitance on the second stage input resistance and on the coupling resistor to the laser. In addition, in both of these places and on the first-stage input there is also a second resistor in series with the capacitor. These resistors will limit the circuit's high frequency gain in the region above 30 MHz. The purpose is to prevent parasitic loop oscillations that can develop at very high frequencies. Also decreasing the resistances may allow a wider bandwidth as long as the loop remains stable. An offset control is also included on the input to op-amp U2. Its purpose is to bias the second amplifier's output such that under steady-state conditions (or for the unlocked state) there is very little current through the coupling resistor. In other words, we adjust the pot so that the amplifier's output is close to the lasers junction voltage. This gives the circuit the advantage that it can be connected to the laser by closing switch SW6 without appreciably perturbing the laser frequency.

The second path, or slow feedback, goes to op-amp U3 (LM741) that controls the voltage sent to the PZT driver for the laser diode cavity. The advantage of this configuration is that the low-frequency corrections are dominated by the large gain in the PZT channel so that the laser current DC level remains constant (large changes in this current can lead to laser mode hops). In fact, under the locked condition, DC level after the first stage should be equal to zero when this stage is configured as an integrator. This highlights one of the aspects of using integrators in these feedback loops - a non zero correction can be applied (after amplifier U3 in

our circuit) while a zero-error signal can be maintained. We also benefit from the increased low-frequency gain in the overall loop transfer function. For added flexibility in this stage, we have included a switch, SW5, across the feedback capacitor, so we can switch between flat gain and a full integrator (as we did with SW3 on the first stage). The PZT driver does not have a polarity switch so we have used a simple inverting amplifier U4 (LM741) following the integrator. We note also that for more accurate locking, amplifier U4 should have its inherent offset adjusted prior to any input. We control the overall loop gain with a potentiometer ($2.5\text{ k}\Omega$) that varies the attenuation between the first and second amplifier stages. A one-turn pot is used to minimize stray capacitance that might limit the feedback bandwidth. The electronic circuit board is located close to the laser, to avoid unnecessary time delays and cable capacitance.

5.4 Locking the Laser and Loop Optimization

In this section we have adopted the procedure mentioned by Fox et al. [22]. After the loop filter is designed, we lock the laser to a feature of the rubidium spectrum. First, we need to compensate any DC offsets in the signal coming from the mixer. With the laser nominally aligned and the output switch SW6 open, the signal at the output of op-amp U1 should yield a low-pass filtered version of the error signal centered at zero volts DC. Any offset from zero can be adjusted with the offset current through switch SW1. We usually check for locking action by closing switch SW6 and turning up the gain knob (with the PZT feedback gain turned off for the moment). An increase in transmission of the signal is an indication that the polarity of the system is correct and the feedback loop is attempting to keep the laser locked to the reference fringe. If the overall sign of the

servo is wrong, the signal will be suppressed and the system will try to lock to the sidebands instead. This situation can be corrected by choosing the opposite slope for the discriminator (i.e., by changing the demodulation phase by 180°). Adjusting the overall gain by turning the potentiometer will give us some clues as to whether more gain is required or not. If the servo seems to be trying to lock, we can then reduce the sweep to zero and the laser should stay in lock for increasing fractions of the sweep. If this is indeed the case, it is a good time to optimize the alignment of the extended cavity diode laser.

If the servo clearly perturbs the laser but no locking action is observed even on the sidebands, it is possible that the gain is too low. We recall that a portion of the servo loop's gain curve is decreasing as f^{-2} , or -40 dB per decade. If the overall loop gain is such that the servo's unity-gain point occurs on this steep slope then no locking will occur. When the laser is locked to the reference peak, increasing the gain past the optimum point will cause a servo oscillation that will be evident on the error signal. Reducing the gain slightly (just below oscillation) provides a good initial setting. In a similar way, the PZT gain can be increased until instability ensues and then reduced slightly. If turning on the PZT gain drives the laser out of lock, the sign of the PZT feedback may need to be reversed. With the PZT gain turned up, the signal observed after the first amplifier stage (U1 in Figure 5.4) should be driven to zero.

In order to switch the laser in and out of lock repetitively, we need some fast way to turn the servo off and back on. Simply switching the error signal off (with SW2) at the first amplifier's input serves to unlock the laser. Switching off the output switch SW6 has the same effect. We keep the PZT integrator switch (SW5 in Figure 5.4) open during the unlocking and locking cycle, so that the laser's PZT driver voltage remains appreciably unchanged.

5.5 Printed Circuit Board (PCB)

We have used Eagle Cadsoft to design and develop a PCB for the feedback circuit. Figure 5.6 displays the PCB of our laser locking circuit. An error signal circuit is also included on the PCB which consists of several RF components from mini-circuits including an RF oscillator, a phase shifter, a low pass filter and a mixer. Most of the components in the circuit are surface mount devices but some of them like pots and resistors are through hole devices. The PCB is designed as a double layer with the ground of the circuit at the bottom layer. Voltage regulators are used that can supply appropriate voltage to the IC's. All the surface mount capacitors are of 50 V rating and the coupling capacitors of $1\ \mu\text{F}$ and $0.1\ \mu\text{F}$ are used in parallel to the power supply pins of the regulators and IC's.

After soldering all the components on the PCB, we check the power supply through the various IC's and circuit components. We then test the functioning of the various RF components, gain and the frequency response of the operational amplifiers. The feedback circuit is tested and we find the various bode plots as desired. Figure 5.7 and Figure 5.8 displays the bode gain plot for the operational amplifiers U1 and U3. The circuit board is now ready to be used for locking the laser and the process mentioned in the previous section (5.4) can be implemented. For further details about the printed circuit board, see appendix A.

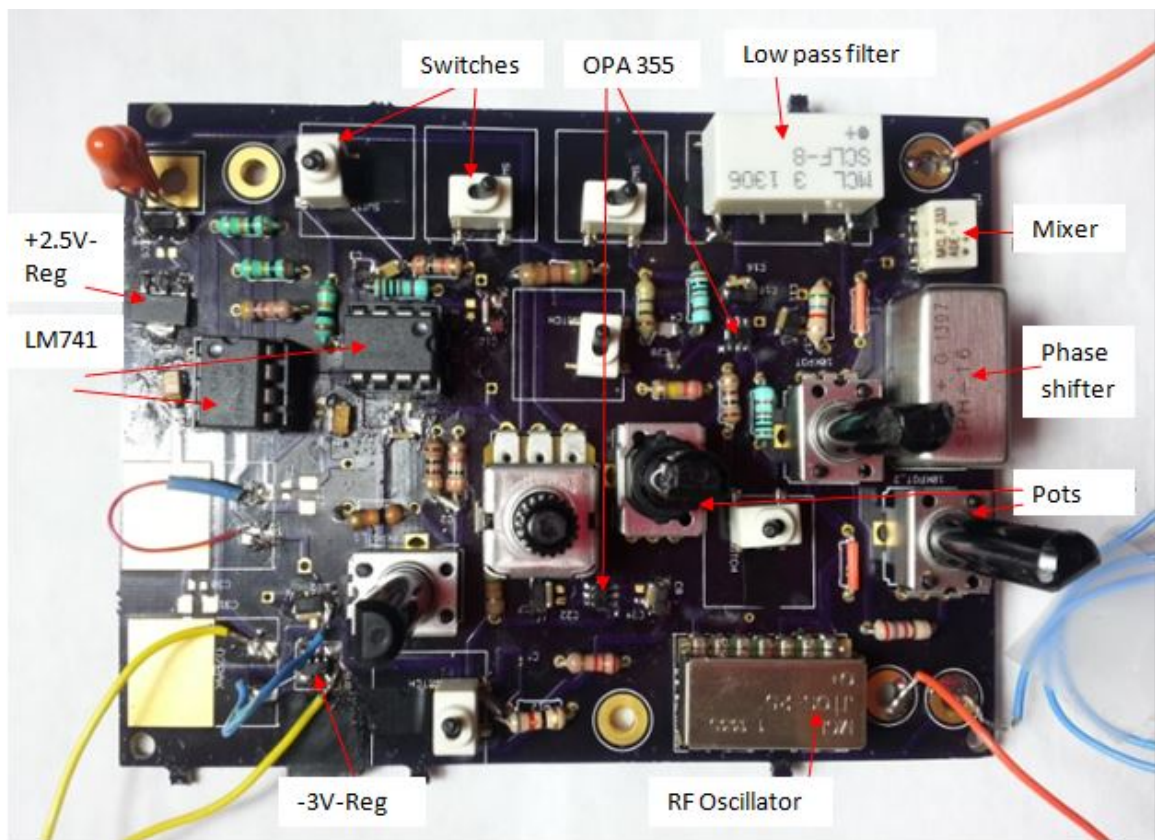


Figure 5.6: Printed circuit board for the feedback loop filter circuit.

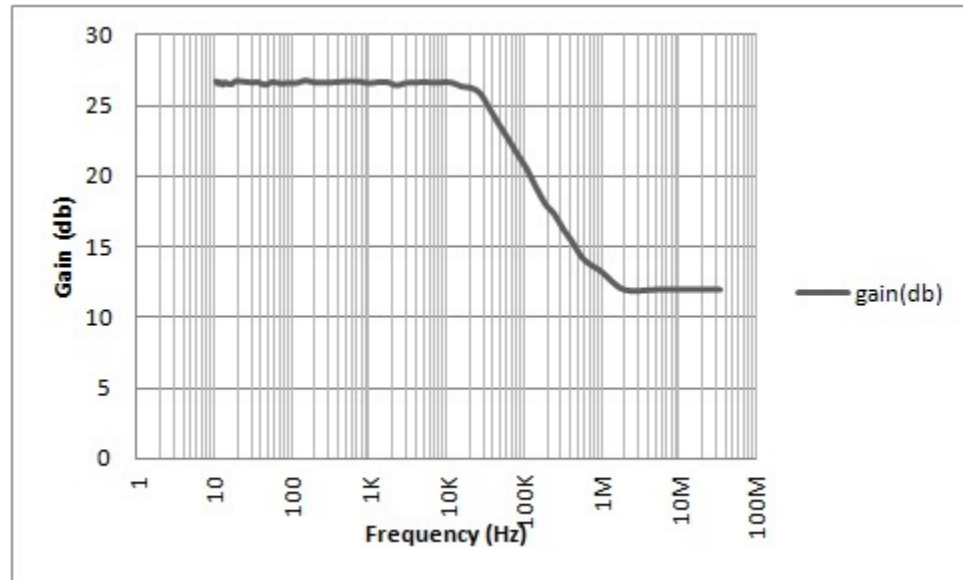


Figure 5.7: Bode gain plot for opamp U1 with SW3 closed.

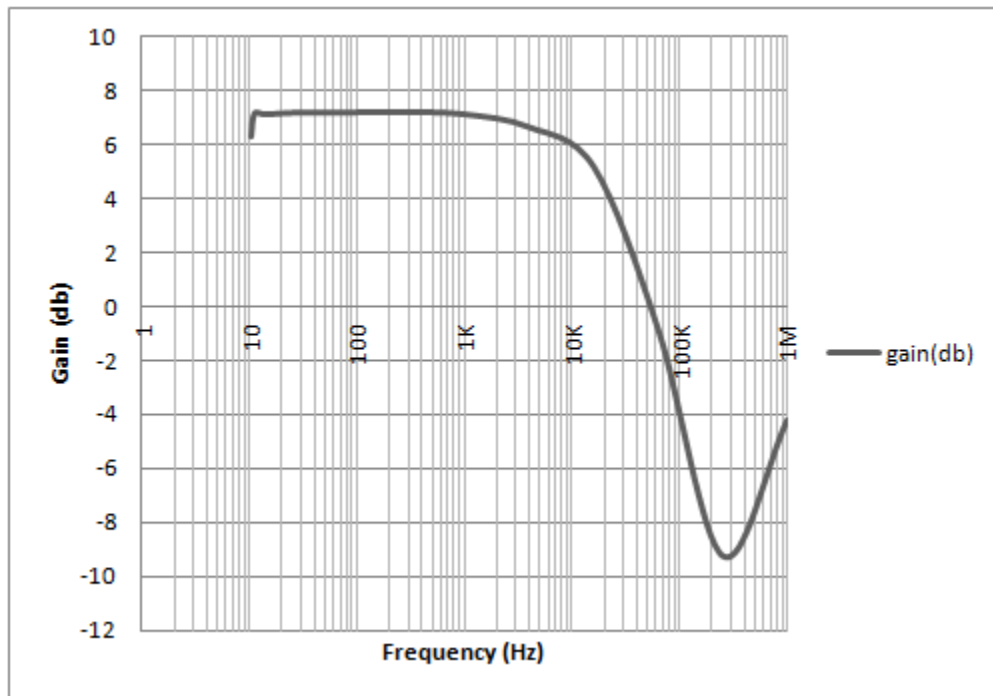


Figure 5.8: Bode gain plot for opamp U3 with SW5 closed.

CHAPTER 6

RESULTS AND CONCLUDING REMARKS

6.1 Results

In this thesis, we have described in some detail a simple approach of locking an extended cavity diode laser to a rubidium absorption spectral line. We designed and fabricated a locking circuit that includes RF components for generating an error signal as well as the feedback loop filter circuit. We have found the overall approach to be quite flexible and yield good results on a fairly short time scale. Figure 6.1 displays the snapshot of an oscilloscope screen depicting an error signal.

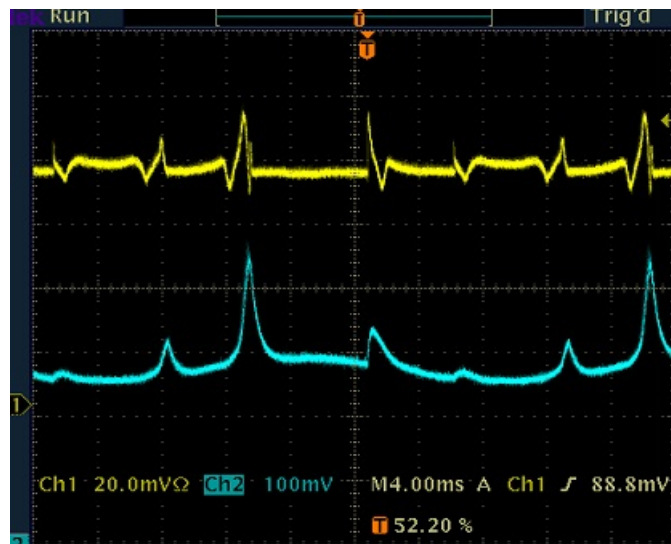


Figure 6.1: The yellow signal (top) is an error signal, the blue signal (bottom) is the resonance of an Rb cell.

In Figure 6.1, the blue signal (bottom) shows the fluorescence produced by the rubidium cell and the yellow signal (top) is the error signal obtained by the circuit

that we designed. The error signal shown in the figure is offset from zero which can be adjusted with the help of the 10 k Ω pot, so that it passes through the average value at the resonant frequency. We optimize the shape of the error signal (refer to Figure 5.2) by changing the phase of the local oscillator and the amplitude of the RF signal modulation.

After following the method mentioned in section (5.4), we are able to lock the laser for a few minutes (4-5 minutes). Initially, locking of the ECDL frequency is done with the current feedback path only and the PZT channel is turned off with the help of the switch SW4. As we increase the gain of the current feedback circuit with the help of the potentiometer, we see a hike in the transmission intensity at a particular value of the laser injection current. We note down this value of current since it can be used for locking in case the system gets unlocked. At this point, the system is locked and we put on the integrator switch for opamp U1. We observe that the transmitted intensity signal stays at a higher level; we record the time the signal stays in the locked condition. After a few minutes, the signal comes down and the system becomes unlocked.

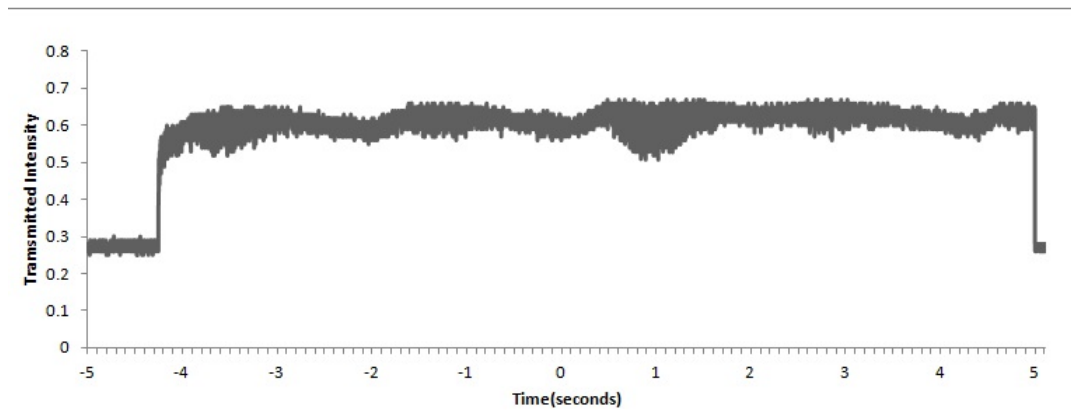


Figure 6.2: Laser frequency locking: transmitted light intensity versus time, representing a lock duration of 9 seconds.

Figure 6.2 displays the plot of the intensity versus time that we obtained while tuning the frequency of the laser with the current path. We can further increase the frequency locking time of an ECDL by turning on the switch of the PZT path. We observe that the polarity of the PZT channel is negative, so we have to use the optional inverter in our feedback circuit of the PZT (switch SW8 has to be closed).

6.2 Concluding Remarks and Future Work

The purpose of this thesis was to develop an extended cavity diode laser that is frequency locked to an atomic transition, at a significantly reduced cost compared to commercially available solutions. We have been successful in characterizing the various frequency parameters (injection current, temperature, and grating feedback) and are able to tune the frequency of the diode laser without the use of expensive electronic devices and circuitry. The cost of a typical commercially available ECDL system is around 10K USD [25], whereas the overall cost of our device is approximately 500 USD. This device can be used in undergraduate and graduate level optics laboratories. We have also designed and built another mount with some modifications to simplify the control system. This new mount was built to reduce mode-hopping and efficiently stabilize the temperature of an ECDL. It satisfies the conditions mentioned in section (2.6) of optimal rotation point to achieve mode-hop suppression. Figure 6.3 displays the set up of our new mount. This new mount has been made from scratch with all the components built in our mechanical workshop. In the future, we can develop a number of these mounts, as well as locking circuits, that can be a useful light source for spectroscopy experiments in our research, laboratory, and courses.

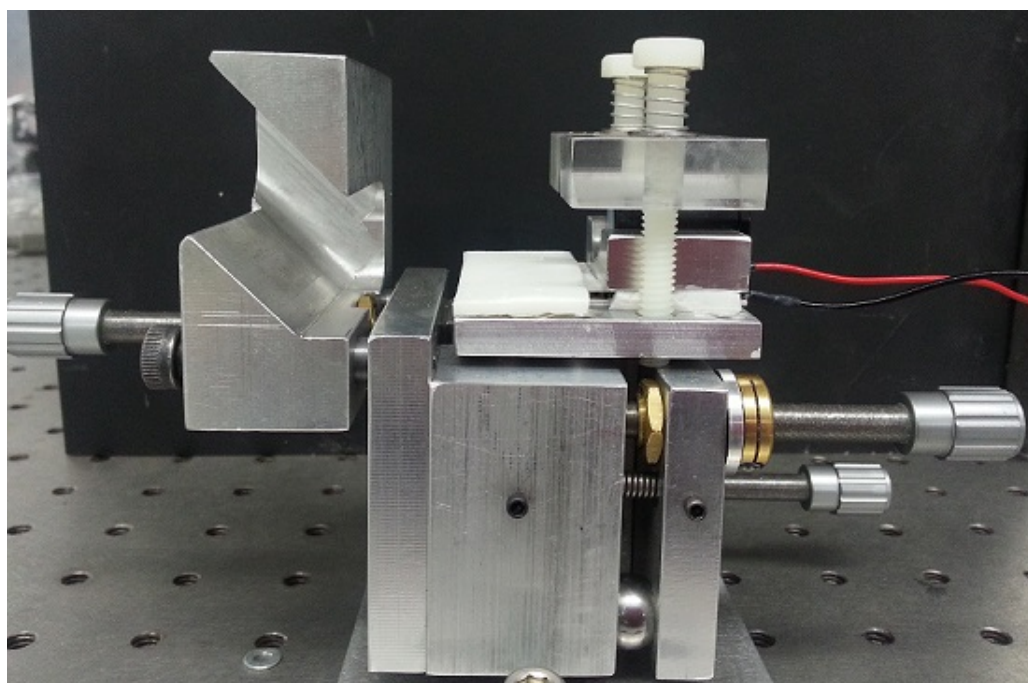


Figure 6.3: New ECDL mount that reduces mode-hop.

BIBLIOGRAPHY

- [1] C. Ye, *Tunable External Cavity Diode Lasers*. World Scientific, 2004.
- [2] M. Schu, *External Cavity Diode Lasers: Controlling Laser Output Via Optical Feedback*. College of William and Mary, 2003.
- [3] W. T. Silfvest, *Fundamentals of Photonics-LASERS*, 2005.
- [4] B. Saleh and M. Teich, *Fundamentals of Photonics*. Wiley Series in Pure and Applied Optics, Wiley, 2007.
- [5] N. Corporation, “Laser Diode Technology,” 2013. [Online; accessed Jan-2014].
- [6] I. Poole, “Laser diode types-radio electronics.”
http://www.radio-electronics.com/info/data/semicond/laser_diode/types-laser-diodes.php, 2013. [Online; accessed Nov-2013].
- [7] J. Crowe and R. Craig *Appl. Phys. Lett.*, vol. 5, p. 72, 1964.
- [8] C. E. Wieman and L. Hollberg, “Using diode lasers for atomic physics,” *Review of Scientific Instruments*, vol. 62, pp. 1–20, Jan. 1991.
- [9] P. Zorabedian, “Tunable external-cavity semiconductor lasers,” in *F. J. Duarte (ed.), Tunable Lasers*, p. 349, 1995.
- [10] A. S. Arnold, J. S. Wilson, and M. G. Boshier, “A simple extended-cavity diode laser,” *Review of Scientific Instruments*, vol. 69, pp. 1236–1239, Mar. 1998.
- [11] C. A. Heredia, “Diode laser with external grating based cavity,” tech. rep., San Luis Obispo, California, 2004.
- [12] B. Azmoun and S. Metz, “Recipe for locking an extended cavity diode laser from the ground up,” tech. rep., Stony Brook University, New york, 2000.
- [13] S. L. Cornish, “Introduction to Diode Lasers.”
http://massey.dur.ac.uk/resources/grad_skills/LaserExpts.pdf, 2007.
 [Online; accessed Aug-2013].
- [14] M. de Labachellerie and G. Passedat, “Mode-hop suppression of littrow grating-tuned lasers,” *Appl. Opt.*, vol. 32, pp. 269–274, Jan 1993.

- [15] H. Tabuchi and H. Ishikawa, “External grating tunable mqw laser with wide tuning range of 240 nm,” *Electronics Letters*, vol. 26(3), pp. 742–743, May 1990.
- [16] F. Favre, “External-cavity semiconductor laser with 15 nm continuous tuning range,” *Electronics Letters*, vol. 22(3), pp. 795–796, Jul 1986.
- [17] L. Levin, “Mode-hop-free electro-optically tuned diode laser,” *Optics Letters*, vol. 27(4), pp. 237–239, Feb 2002.
- [18] M. Juarez and P. Oxley, “The Use of a Lock-In Amplifier to Stabilize the Frequency of a Diode Laser,” Master’s thesis, College of the Holy Cross-Massachusetts, 2009.
- [19] D. University-UK, “Doppler-Free Saturated Absorption Spectroscopy-Laser Spectroscopy.” [Online; accessed Sep-2013].
- [20] D. of Physics-University of Florida, “Saturated Absorption Spectroscopy.” http://www.phys.ufl.edu/courses/phy4803L/group_III/sat_absorbtion/SatAbs.pdf, 2010. [Online; accessed Sep-2013].
- [21] C. University-California, “Ph 77 Advanced Physics Laboratory-Atomic and Optical Physics-Diode Laser Characteristics.” <http://www.its.caltech.edu/~ph76a/satabs.pdf>. [Online; accessed Jul-2013].
- [22] R. W. Fox, C. W. Oates, and L. W. Hollberg, “1. stabilizing diode lasers to high-finesse cavities,” in *Cavity-Enhanced Spectroscopies* (R. D. van Zee and J. P. Looney, eds.), vol. 40 of *Experimental Methods in the Physical Sciences*, pp. 1 – 46, Academic Press, 2003.
- [23] M. C. R. Hoogeveen, “Stabilizing a diode laser to an external reference,” Master’s thesis, KVI-Kernfysisch Versneller Instituut, 2003.
- [24] I. DesignSoft, “TINA-V10,” 2012. [Online; accessed Jul-2013].
- [25] I. Thorlabs, “Thorproducts.” <http://www.thorlabs.us/thorproduct.cfm?partnumber=TLK-L780M>. [Online; accessed Mar 6-2014].

APPENDIX A

PRINTED CIRCUIT BOARD

This section describes in some detail, the printed circuit board (PCB) of our locking circuit. We design the schematic of the circuit in Eagle cadsoft free student version that allows us to generate a board layout of 4 inches by 3 inches. Our PCB is a double sided board with ground plane as the bottom layer. Figure A.1 shows

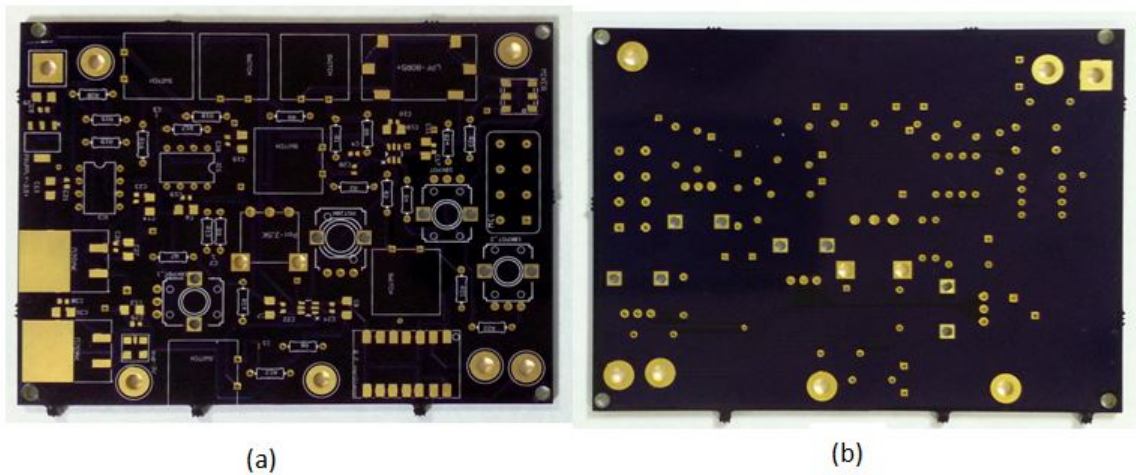


Figure A.1: PCB Board (a) front panel and (b) back panel.

the front and back panel of our PCB, whereas Figure A.2 displays the board layout with traces in blue and red. The blue traces show the connections at the bottom layer. There are six circular mounting pads (3mm diameter) for the external connections such as + supply, - supply, V(laser diode current), V(PZT), V(Photodiode signal input) and RF oscillator output. The square mounting pad is for connecting the circuit ground with the external ground. The locking circuit consists of two parts, the error signal circuit and the feedback loop filter circuit.

The error signal circuit includes components like an RF oscillator, a phase shifter, a frequency mixer and a low pass filter. A surface mount voltage controlled oscillator (minicircuit model-JTOS-25+) is used to generate signals of frequency 15 MHz.

The maximum tuning voltage for this oscillator is +12 V, so we connect a 10 k Ω pot

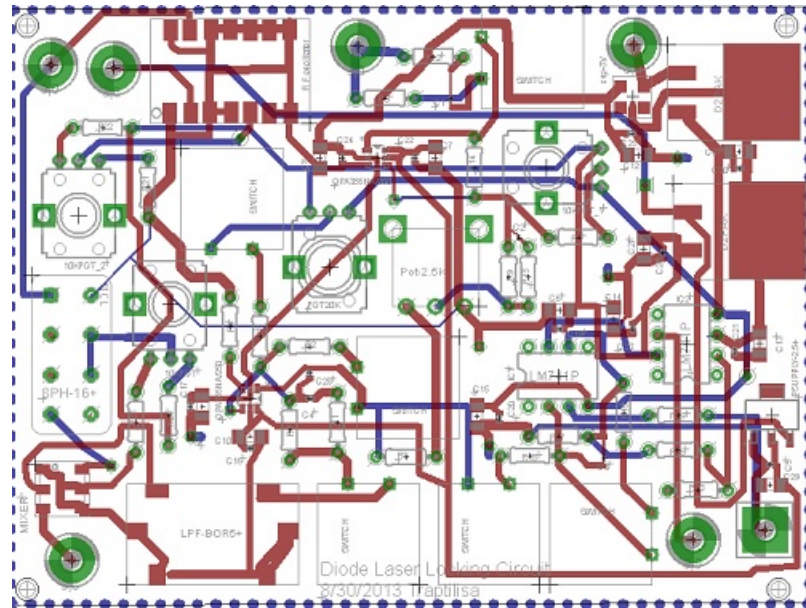


Figure A.2: Board layout with traces.

across the tuning voltage pin of the oscillator and adjust it to set the oscillator frequency to its nominal value of 15 MHz. The phase shifter in the circuit is a minicircuit SPH-16+ (50 Ω , 180° voltage variable) and operates at 13-16 MHz frequency range. A surface mount minicircuit (ADE-1+) frequency mixer of level 7 (LO power+7 dBm) is used to produce new signals at the sum ($f_1 + f_2$) and difference ($f_1 - f_2$) of the original frequencies f_1 and f_2 . A low pass filter (minicircuit model-SCLF-8+) that has a pass band above the unity gain frequency of the feedback circuit but below the modulation frequency is used to filter the error signal. The circular mounting pad on the upper left corner provides the RF signal for frequency modulation, i.e., we connect an external wire from the pad to the laser

diode current injection terminal via a bias tee.

The feedback loop filter circuit is designed using the schematic shown in Figure 5.4. The low pass filtered version of the error signal goes to the feedback amplifier circuit containing an opamp 355, which is a surface mount and has a SO-23-6- package PCB layout. The amplified signal from this opamp splits into two channels. One channel goes to another opamp 355 for further gain in the signal and the output of which goes to mounting pad V(laser diode current) for tuning the frequency through current injection. The other channel goes to opamp LM741 which is a through hole device and has a 8-DIP package attached to an 8 pin socket. The output of the signal from this channel goes to the mounting pad V(PZT). There are five potentiometers in the circuit. 10 k Ω pots are used to change the phase of the signal at the phase shifter and set the DC offset of the error signal. Another 20 k Ω pot is used to set the DC offset of the operational amplifiers. To increase the gain of the signal in the current path, a pot of 2.5 k Ω is used in the circuit. The potentiometers are soldered through hole devices with 5 pins, out of which 2 pins are soldered for mechanical support. Two voltage regulators (digikey part-MIC5270-3.0YM5 TR) of SOT-753 package and (digikey partl-ZLDO1117G25TA) SOT-223-3 package are used to provide -3 V and +2.5 V supply to the OPA 355, whereas the +15 V and -15 V supply is provided to the LM 741 opamps. All the resistors used in the circuit are through hole devices while the capacitors are surface mounts of case style C1206. Six toggle switches are used in the circuit to control the various functions and operations of the circuit. We also add 4 large mounting holes in the corners of the board to mechanically mount the board (with screws).